Accepted Manuscript

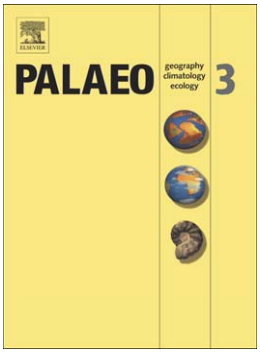

An enigmatic kilometer-scale concentration of small mytilids (Late Miocene, Guadalquivir Basin, S Spain)

Julio Aguirre, Juan C. Braga, José M. Martín, Ángel Puga-Bernabéu, José N. Pérez-Asensio, Isabel M. Sánchez-Almazo, Luciana Génio

PII: S0031-0182(15)00375-2
DOI: doi: 10.1016/j.palaeo.2015.07.015
Reference: PALAEO 7363

To appear in: *Palaeogeography, Palaeoclimatology, Palaeoecology*

Received date: 17 March 2015
Revised date: 7 July 2015
Accepted date: 10 July 2015

Please cite this article as: Aguirre, Julio, Braga, Juan C., Martín, José M., Puga-Bernabéu, Ángel, Pérez-Asensio, José N., Sánchez-Almazo, Isabel M., Génio, Luciana, An enigmatic kilometer-scale concentration of small mytilids (Late Miocene, Guadalquivir Basin, S Spain), *Palaeogeography, Palaeoclimatology, Palaeoecology* (2015), doi: 10.1016/j.palaeo.2015.07.015

This is a PDF file of an unedited manuscript that has been accepted for publication. As a service to our customers we are providing this early version of the manuscript. The manuscript will undergo copyediting, typesetting, and review of the resulting proof before it is published in its final form. Please note that during the production process errors may be discovered which could affect the content, and all legal disclaimers that apply to the journal pertain.

ACCEPTED MANUSCRIPT

An enigmatic kilometer-scale concentration of small mytilids (Late Miocene, Guadalquivir Basin, S Spain)

Julio Aguirre[1*], Juan C. Braga[1], José M. Martín[1], Ángel Puga-Bernabéu[1], José N. Pérez-Asensio[2], Isabel M. Sánchez-Almazo[3], and Luciana Génio[4]

[1] Dpt. Estratigrafía y Paleontología, Facultad de Ciencias, Fuentenueva s/n Universidad de Granada, 18071 Granada, Spain

[2] Section of Earth and Environmental Sciences, University of Geneva, Rue des Maraîchers 13, 1205 Geneva, Switzerland

[3] Centro de Instrumentación Científica, Fuentenueva s/n, Universidad de Granada, 18071 Granada, Spain

[4] Centro de Estudos do Ambiente e do Mar, Dpt. de Biologia, Universidade de Aveiro, Campus Universitário de Santiago, 3810-193 Aveiro, Portugal

* Corresponding author: jaguirre@ugr.es

ACCEPTED MANUSCRIPT

ACCEPTED MANUSCRIPT

Abstract

Upper Miocene heterozoan carbonates crop out extensively in a NE-SW-trending belt (42 km long and 1.5–8 km wide) along the so-called El Alcor topographic high, from Carmona to Dos Hermanas (Seville, S Spain). These carbonates formed at the southern active margin of the Guadalquivir Basin, the foreland basin of the Betic Cordillera. They change to marls basinward (NE) and to sands landward (SE and SW). Therefore, carbonate production was constrained to a limited area in an otherwise siliciclastic shelf. The carbonates (up to 40 m thick) overlie a gradually coarsening-upward succession of marls followed by silts and sandstones. The carbonate sequence can be divided into three subunits corresponding, from bottom to top, to lowstand, transgressive, and highstands system tracts deposits. The lower subunit, exhibiting extensive trough cross-bedding, is interpreted as a shallow-water bar deposit. The intermediate subunit onlaps underlying sediments and was deposited in deeper, low-turbulence conditions. The upper subunit deposits accumulated in a well-oxygenated outer platform based on benthic foraminiferal assemblages. The presence of hummocky and swaley cross-stratification in these latter deposits suggests that they were affected by storms. Pervasive fluid-escape structures are also observed throughout the carbonates.

The three subunits consist of bioclastic packstones to rudstones made up of abundant fragments of small mytilids. Isotopic data from serpulid polychaete *Ditrupa* tubes show ^{13}C-depleted values (up to -16.1‰), whereas $\delta^{18}O$ yields normal marine values. Additional isotopic data on shells of scallops, oysters, and small mussels, as well as bulk sediment, show diagenetic alterations. Based on actualistic examples of massive concentrations of mussels, the nearly monospecific composition of the El Alcor deposits, together with negative $\delta^{13}C$ values of *Ditrupa* tubes, indicates that cold seeps

ACCEPTED MANUSCRIPT

presumably promoted carbonate formation. However, the absence of typical features of cold-seep deposits, such as authigenic carbonates mediated by anaerobic bacterial activity and the typical chemosynthetic shelly organisms, makes the large carbonate body of El Alcor an unusual cold-seep deposit.

Keywords. Cold seep; heterozoan carbonates; mussels; Carmona; El Alcor.

ACCEPTED MANUSCRIPT

ACCEPTED MANUSCRIPT

1. Introduction

Light, temperature, and nutrients are thought to be the major factors controlling associations of benthic organisms that produce carbonate particles in marine environments and therefore types of carbonate sediments (e.g. James, 1997; Mutti and Hallock, 2003). Photozoan carbonates form only in well-illuminated, warm shallow-water settings, whereas heterozoan carbonates, produced mainly by light-independent organisms, can accumulate in a wide range of water temperatures and depths (James, 1997; Schlager, 2003). Known heterozoan carbonates are made up of skeletal particles of heterotrophic invertebrates, including in some cases coralline red algae.

Bivalves are among the most abundant components in the heterozoan carbonates. Of these, mussels (Bivalvia: Mytilidae) are able to produce dense concentrations (the so-called mussel beds, mussel aggregations, mussel reefs, mussel bioherms) in different mid- and high-latitude aquatic ecosystems (e.g. Bertness and Grosholz, 1985; Commito and Dankers, 2001; Gutiérrez et al., 2003), leading to massive carbonate accumulations. Based on data of biomass production of *Mytilus edulis* from western Sweden (Loo and Rosenberg, 1983) and the Wadden Sea (Asmus, 1987), Steuber (2000) estimated a carbonate production rate ranging from 2 to 6.5 kg per m^2 and year. In soft-bottom marine settings, kilometer-scale mussel beds can be found in a very wide range of water depths, from marshes and subtidal settings to deep abyssal planes. In very shallow waters, crowded concentrations of the blue mussel (*Mytilus edulis*) in tidal flats and subtidal settings are well known (Dittmann, 1990; Commito and Dankers, 2001; Commito et al., 2006; Folmer et al., 2014). Additionally, dense aggregations of the ribbed mussel (*Geukensia demissa*) have been described in the seaside margin of salt marshes from the western North Atlantic (Bertness, 1984;

ACCEPTED MANUSCRIPT

Bertness and Grosholz, 1985; Franz, 1993, 1996, 2001). In subtidal conditions, from a few meters deep down to ~100 m, the horse mussel (*Modiolus modiolus*) forms elongated accumulations (bioherms/reefs) in the Northern Atlantic (Magorrian and Service, 1998; Wildish et al., 1998, 2009; Lindenbaum et al., 2008; Gormley et al., 2013; Elsäßer et al., 2013). Finally, chemosynthetic mytilids can also be major colonizers in hydrothermal vents and cold-seep areas (Paull et al., 1992; Aharon, 1994; Pichler and Dix, 1996; Sibuet and Olu, 1998; Schlager, 2003; Levin, 2005; Conti and Fontana, 2005; Campbell, 2006; Roberts et al., 2010; Taviani, 2010).

Massive accumulations of mussels form a kilometer-scale carbonate body along the so-called El Alcor area (Seville, SW Spain) (Fig. 1). These carbonates consist of rudstones-packstones of mussel fragments and are completely surrounded by siliciclastics. They extend along the outer fringe of a terrigenous Late Miocene ramp on the active margin of the Atlantic-linked Guadalquivir Basin (S Spain). We describe these enigmatic heterozoan carbonates, studying the nature of the major carbonate producer and analyzing stable isotopes of the carbonates in order to decipher the paleoenvironmental context in which they formed. Comparisons with present-day massive accumulations of mytilids, together with geochemical results and taphonomic observations, suggest that the El Alcor carbonates might most likely represent unusual cold-seep deposits.

2. Location and geologic setting

The studied deposits crop out in a SW-NE trending belt 42 km along the so-called El Alcor, a topographic high extending from southwest of Dos Hermanas to Carmona (Seville, SW Spain) (Fig. 1). The width of the carbonate belt increases

ACCEPTED MANUSCRIPT

southwestward: 1.5 km in Carmona, about 3.5 km in Alcalá de Guadaira, and up to 8 km in Dos Hermanas (Fig. 1). These carbonates change laterally to marls to the north-northwest (basinward) and to sands to the southeast, and southwest (landward) (Viguier, 1974).

The carbonates were deposited at the active southern margin of the Guadalquivir Basin (S Spain), the SW-NE elongated foreland basin of the Betic Cordillera (Fig. 1). During the Middle Miocene (late Serravallian), the Guadalquivir Basin was part of a corridor formed between the passive Iberian Massif, to the north, and the active Betic Cordillera to the south, connecting the Atlantic Ocean with the Mediterranean Sea (Braga et al., 2010). This marine passage was closed at its northeastern end, the so-called North Betic Strait, in the earliest Tortonian (Martín et al., 2009; Braga et al., 2010). As a result, the Guadalquivir Basin evolved into a wide embayment open to the Atlantic Ocean to the southwest (Martín et al., 2009). This embayment was later filled with Upper Miocene to Upper Pliocene sediments (Roldán, 1995; Aguirre et al., 1995; Sierro et al., 1996; Braga et al., 2002; González-Delgado et al., 2004), prograding from the northeast to the southwest along the central part of the basin. Olistoliths from the thrusting front of the Betic Cordillera mixed with the autochthonous sedimentation in the course of the Miocene. Resulting olistostrome deposits occur at the southern margin of the basin, reaching up to its axis (Sanz de Galdeano and Vera, 1992) (Fig. 1).

The El Alcor carbonates occur at the top of a gradually coarsening-upward succession consisting of blue marls at the base, followed by silts and sands (Perconig, 1968; Viguier, 1974; Berggren and Haq, 1976). The coexistence of planktonic foraminiferal species *Globorotalia margaritae* and *Globorotalia miotumida* group in silts below the carbonates, as well as in the silts intercalated in the carbonates indicates that the studied deposits are late Messinian in age.

ACCEPTED MANUSCRIPT

The whole succession unconformably overlies olistostrome deposits (Fig. 1), mostly made up of diatomitic marlstones (locally called Albarizas or Moronitas) from the Carmona nappe (Perconig and Martínez-Díaz, 1977).

3. Methods

We mapped the El Alcor carbonate body and selected the four best-exposed localities for detailed logging and sampling (Figs. 1 and 2). Seven samples were collected in fine-grained sediments both immediately below and intercalated with the carbonates in order to study benthic foraminiferal assemblages. After sieving through a 63 μm sieve, each sample was split into equal subsamples. These subsamples were then sieved through a 125 μm mesh and 300 benthic foraminifers were counted and identified from this size fraction to gather census data of the microfossil assemblages. We also studied 32 thin sections for microfacies and petrographic analyses. Semi-quantitative data of siliciclastic, bioclastic, and void contents were estimated using the Baccelle and Bosellini's (1965) charts.

Carbon and oxygen stable isotope analyses were carried out on bulk rock and skeletal carbonates of different groups of organisms: small mussels, scallops, the oyster *Neopycnodonte cochlear*, benthic foraminifera, and the serpulid polychaete tubes *Ditrupa*. The analysed samples were collected both from the carbonates (bulk rock, pectinids, *Neopycnodonte cochlear* and small mussels) as well as from intercalated silts and fine-grained sands (*Ditrupa* and benthic foraminifera) (Fig. 2). Bulk rock samples include bioclastic carbonates and cemented sandy packstones collected around fluid-escape structures. Remains of matrix and/or possible coatings of calcite adhered to the shells of mussels, scallops, oysters, and worm tubes were removed using a microdrill.

ACCEPTED MANUSCRIPT

No previous isotopic studies are available on *Ditrupa* tubes. To test whether this serpulid precipitates its skeleton in isotopic equilibrium with marine water, we measured C and O stable isotopes in modern *Ditrupa arietina* tubes from the western Mediterranean: one shell off Sant Feliu de Gruixols (Barcelona, NE Spain) collected at 10 m water depth, and three shells off Cabo de Gata (Almería, SE Spain) sampled at 60 m water depth.

Isotopic data from benthic foraminiferal tests were recorded from two epifaunal species (*Biasterigerina planorbis* and *Cibicides refulgens*) and two infaunal species (*Reussella spinulosa* and *Bolivina spathulata*) collected in each sample. In one sample, we analysed *Cibicides dutemplei*, *Planulina ariminensis*, *Melonis pompilioides*, and *Uvigerina peregrina* instead, due to the absence or low abundance of the aforementioned four species.

All samples were ultrasonically cleaned and washed in demineralized water. The organic matter was removed with 3% oxygen peroxide in an ultrasonic bath, rinsed with methanol, and dried at 40ºC overnight. The clean, dry samples were reacted in 103% orthophosphoric acid at 90°C in a multicarb device connected to dual inlet Isoprime mass spectrometer located at the Centro de Instrumentación Científica of the University of Granada. Analytical precision based on replicate analyses of NBS19 and NBS18 was better than ±0.05 and ±0.08‰ for C and O, respectively. Oxygen and carbon isotope ratios are expressed relative to VPDB.

The percentage of bioclasts per rock volume and fossil packing were estimated at the outcrop using the templates of Kidwell and Holland (1991). Additionally, some qualitative taphonomic data on articulation, fragmentation, abrasion, and dissolution were taken in the field and then checked in high-resolution pictures and under the microscope.

ACCEPTED MANUSCRIPT

4. Stratigraphy

The El Alcor carbonate succession, up to 20 m thick, can be divided into three subunits, which are well exposed in the Carmona Quarry section, located in an abandoned quarry NE of Carmona (Fig. 3). The lower subunit, 8-10 m thick, is represented only in this section (Fig. 2). This subunit shows a bar morphology and consists of bioclastic rudstone with 15-20% of quartz (Figs. 2 and 3). The lower part shows plane parallel beds up to 2.5 m thick, whereas meter-scale trough cross-bedding, locally slumping westward (N240ºE) appears in the upper part (Figs. 4A and B). Fluidization structures, such as deformed beds and pipe-like structures affect these deposits. The top of the subunit is an irregular indurated surface.

The intermediate subunit, up to 3 m in thickness, onlaps the irregular surface on top of the underlying subunit (Figs 2 and 3). The intermediate subunit consists of well-bedded packstones intercalating thin silt beds (Fig. 2). Internally, carbonate beds show parallel lamination (Fig. 3). Locally, soft clasts made up of whitish-grey marls are embedded in the silty intercalations. The intermediate subunit also occurs at the Carmona Antena and Carmona Fútbol sections (Fig. 2). In the former, this subunit is made up of silt with abundant *Ditrupa* worm tubes. The carbonate content increases upward, changing to intensively bioturbated silty/sandy packstones at the top of the subunit (Fig. 4C). In the Carmona Fútbol section, the intermediate subunit (2-3 m thick) is characterized by silt intercalating plane parallel beds of fine-grained sandy packstones (Figs 2 and 4D). The terrigenous content of the packstone beds can be up to 60%. The carbonate content increases upward in the subunit with a concomitant thinning of the

ACCEPTED MANUSCRIPT

sandy packstone beds. As in the Carmona Antena section, burrowing is intense in the uppermost part of the subunit.

The upper subunit is the best developed in the Carmona Quarry section and can be traced continuously throughout the quarry (Fig. 3). It consists of bedded sigmoidal clinoforms that prograde to the NNW, dipping up to 15º and downlapping on the underlying subunits (Fig. 3). The thickness of each carbonate bed and sediment size decrease downslope. These are packstones to rudstones with thin, silt to fine-grained sand intercalations. Carbonate beds contain from 20 to 40% terrigenous particles (quartz grains). Some sandy beds include soft clasts consisting of grey marls, in the lower part of the subunit. Sedimentary structures change upwards within each bed, with parallel lamination at the base, grading into pervasively bioturbated sediments in the middle. To the WNW, the beds are pervasively deformed by fluid-escape structures, such as dishes and pillars (Fig. 5).

At the Carmona Antena and Carmona Fútbol sections, the upper subunit consists of packstones to rudstones showing poorly defined plane parallel bedding gently dipping WNW (Fig. 2). The thickness of these carbonates remains roughly constant between 9 and 10 m along the El Alcor high. A silty bed, up to 0.5 m thick, is intercalated in the middle of the carbonates (Fig. 2). At the Carmona Fútbol section, the topmost 3 m of the upper subunit shows hummocky and swaley cross-stratification (Figs 2 and 4E).

The upper subunit can be seen along the El Alcor high at least up to Mairena del Alcor, SW of Carmona (Fig. 1). From this locality to the southwest, the carbonates cannot be laterally followed continuously, in part due to quarrying, but crop out again in the vicinity of Alcalá de Guadaira (Fig. 1). Here, in the Alcalá de Guadaira section along the Guadaira River, the upper subunit is up to 40 m thick (Fig. 2). The lower half

ACCEPTED MANUSCRIPT

of the subunit shows well-defined flat parallel bedding. Low-angle, meter-scale swaley cross stratification is overlain by decimeter and meter-scale bidirectional trough cross-bedding in the upper part of the carbonates.

5. Faunal components of El Alcor carbonates

The El Alcor carbonates are composed almost exclusively of fragments of small mytilid shells comprising up to 90–95% of the skeletal components and up to 50% of the rock volume (Fig. 6A). Subordinate elements are scallops (identifiable as *Pecten* sp., *Aequipecten opercularis*, and *A. scabrella*), oysters (*Neopycnodonte cochlear*), and *Ditrupa* worm tubes. *Ditrupa* locally forms dense concentrations in the silts below the carbonates as well as in the intercalated silty bed in the upper subunit.

The small representatives of the family Mytilidae appear as sharp fragments (Figs. 6A-6C), although complete shells are also visible (Figs. 6D-6E). Mytilid shells are small (up to 3.5 cm in maximum length), thin, and elongated (Figs. 6B-6E), sometimes kidney shaped. The umbo is anterior, slightly subterminal, and prosogyrous. The outer surface is smooth, with only commarginal growth lines (Figs. 6B-6D). As in other representatives of the family (modiolins and bathymodiolins), the hinge is edentulous (Wilson, 1998) (Fig. 7A). The shell of recent mytilid consists of an inner aragonitic layer, commonly of nacre microstructure, and an outer layer of various combinations of calcitic and/or aragonitic prismatic (simple prismatic, fibrous prismatic, spherulitic prismatic) and homogeneous microstructures (Taylor et al., 1969; Carter, 1990; Génio et al., 2012). The El Alcor mussels show two layers: the external one is preserved with a fibrous prismatic microstructure made up of calcite, while the internal

ACCEPTED MANUSCRIPT

nacre layer is dissolved and has been often replaced by blocky, mosaic sparry calcite (Figs. 7B-7E).

Based on morphological, mineralogical, and microstructural features, the El Alcor mytilids share similarities with small mussels found typically in chemosynthetic habitats, such as species of the genera *Idas* and *Adipicola*, as well as some of the evolutionary significant units (ESU) of Lorion et al. (2010), included in the subfamily Bathymodiolinae (Lorion et al., 2010; Génio et al., 2012; Ritt et al., 2012). The taxonomy of these mussels is still under debate and a revision of genus and species definitions has been proposed but not yet formally accepted (e.g. Génio et al., 2012; Thubaut et al., 2013). Moreover, shell conservatism and morphological convergences hamper a precise identification of fossil specimens (Génio et al., 2012). Modioliform shells with outer fibrous prismatic and inner nacre microstructures are also included in the genera *Modiolus* and *Amygdalum* of the subfamily Modiolinae (Carter, 1990; Génio, 2010). Finally, the absence of additional anatomical features (e.g. muscle scars) hinders the generic classification of the El Alcor mytilids within the subfamilies Modiolinae or Bathymodiolinae.

Taking into consideration that the taxonomy of the mussels that constitute the main components of the El Alcor carbonates is not definitively resolved, we herein refer to them as small mytilids.

Regarding benthic foraminiferal assemblages, *Biasterigerina planorbis* and *Cibicides refulgens* are the most abundant, representing more than 40% of the total assemblages, followed by *Lobatula lobatula*, *Hanzawaia boueana*, and *Reussella spinulosa* (Table 1). Foraminiferal assemblages of the soft clasts found in the intermediate subunit in the Carmona Quarry section (CCANT-6) are dominated by

ACCEPTED MANUSCRIPT

Planulina ariminensis and *Cibicides pachyderma*. Other species of paleobathymetric significance present in the soft clasts are *Cibicides dutemplei* and *Pullenia bulloides*.

6. Geochemical results

Isotope results are based on samples collected from carbonates, the silty bed intercalated in the upper subunit, and from silts intercalated in the intermediate subunit (Table 2; Fig. 2). Carbon isotope values range from +1.32‰ to -16.1‰, while $\delta^{18}O$ ranges from +1.43‰ to -5.92‰ (Table 2; Fig. 8). The most negative $\delta^{13}C$ values correspond to tubes of the serpulid worm *Ditrupa* (Table 2; Fig. 8). Present-day *D. arietina* from normal marine waters of the western Mediterranean shows normal carbon (ranging from +1.48‰ to +1.80‰) as well as oxygen (from +3.24‰ to +3.54‰) isotope values (Table 2; Fig. 8).

7. Discussion

7.1. Paleoenvironmental interpretation

Based on stratal geometry and facies interpretation, the three subunits of the El Alcor carbonates, from bottom to top, are attributed, respectively, to the lowstand, transgressive, and highstand systems tracts of a depositional sequence (Fig. 9).

The spatial restriction of the lower subunit to the Carmona Quarry section and its geometry suggests that it may represent a bar. Pervasive trough cross-bedding indicates that the bar formed in a high-energy setting. Synsedimentary deformation is evidenced by slumps, deformed cross beds, and fluid-escape structures. The irregular indurated

ACCEPTED MANUSCRIPT

surface at the top of the lower subunit is a slightly eroded hardground that represents a transgressive surface.

The geometry of the intermediate subunit suggests that onlapping wedges of packstone beds adapted to the irregular surface on top of the lower subunit during a subsequent relative sea-level rise. The fine-grained size of the sediment and their ubiquitous parallel-lamination internal structure indicate that this subunit was deposited under deeper, low-energy conditions. In the Carmona Antena and Carmona Fútbol sections, the intermediate subunit is represented by fine-grained sediments intensely bioturbated in the upper part. During maximum flooding conditions, sedimentation rate is usually low, favoring the pervasive colonization of the sea bottom by burrowers (Dam, 1990; Bromley, 1990; Fürsich et al., 1991; Lewis and Ekdale, 1992; Kidwell, 1993; Aguirre, 1995, 2000).

The upper subunit in the Carmona Quarry section prograded to the NNW and downlapped the previous subunits. The presence of hummocky and swaley cross-stratifications, as observed in the Carmona Fútbol and Alcalá de Guadaira outcrops, indicate reworking due to storms and, therefore, deposition above the lower limit of the storm-wave base, at least in some periods. Sedimentary structures change to trough cross-bedding up in the Alcalá de Guadaira section, denoting a shallowing-upward trend. Pervasive deformation structures (deformed strata, pipe-like structures, dishes, and pillars) in the Carmona Quarry section points to significant fluid mobilization throughout the sediments.

Benthic foraminiferal assemblages are dominated by species preferentially inhabiting outer-platform settings. Berggren and Haq (1976) interpreted the microfossil assemblages immediately below the El Alcor carbonates as having formed in water depths of 60 to 100 m, which is consistent with our findings. Dense clusters of *Ditrupa*

ACCEPTED MANUSCRIPT

and presence of *Neopycnodonte cochlear* are found in the fine-grained sediments immediately below the carbonates of the upper subunit. Crowded populations of *Ditrupa* and of *Neopycnodonte cochlear* are common in the same range of water depth on eastern Atlantic platforms (Le Loc'h et al., 2008; Wisshak et al., 2009).

7.2. Origin of the El Alcor carbonates

The El Alcor heterozoan carbonates constitute a large body that formed offshore the southern margin of the Guadalquivir Basin. They appear as a narrow belt surrounded by siliciclastic marine deposits: marls to the NW (basinward) and sands to the SE, and SW (landward) (Fig. 1) (Viguier, 1974). A striking feature of these carbonates, previously highlighted by Viguier (1974), is the homogeneity in skeletal composition throughout the entire area. This constancy indicates that particular conditions were necessary to trigger and maintain uniform carbonate production in an area of the basin in an otherwise terrigenous shelf.

As discussed above, the studied deposits are made up almost exclusively of small mytilids that accumulated in a carbonate platform. The taxonomic attribution of these mytilids is still unresolved, but an actualistic approach can help to understand the origin of the El Alcor carbonates. Dense aggregations of present-day mytilids at a water-depth range similar to those of the El Alcor small mytilids are horse mussel reefs. Other modiolin species with distributions extending from shelf to abyssal depths are classified in the genus *Amygdalum*. Finally, bathymodiolin mussel beds are found at chemosynthetic habitats at depths ranging from a few hundred to 4,000 m (Kiel and Tyler, 2010; Dando, 2010; Lorion et al., 2013).

ACCEPTED MANUSCRIPT

Large concentrations of the horse mussel *Modiolus modiolus* appear at the Bay of Fundy (NE Canada) and Strangford Lough (N Ireland) (Magorrian and Service, 1998; Wildish et al., 1998, 2009; Lindenbaum et al., 2008; Gormley et al., 2013; Elsäßer et al., 2013). These bioconstructions form kilometer-scale elongated structures, 1-3 m in height, oriented perpendicular to sand waves from shallow subtidal (5 m) down to about 100 m water depth, being 20-40 m the preferable bathymetric distribution (Elsäßer et al., 2013). Several ecological studies have shown that these bioconstructions constitute diversification hot spots and *M. modiolus* acts as an ecological engineer (Ress et al., 2008; Sanderson et al., 2008; Gormley et al., 2013; Elsäßer et al., 2013). By contrast, in our study case, fossil assemblages in the El Alcor carbonates are nearly monospecific, as the preserved shelly fauna is dominated almost exclusively by small mytilids (90-95% of the assemblage). Temperature is another controlling factor in horse mussel reef distribution, limited to 7-10ºC (Wildish and Fader, 1998; Gormley et al., 2013). However, oxygen isotope data from coeval deposits in the western edge of the Guadalquivir Basin show a progressive warming of both superficial and deep waters during the late Messinian (Pérez-Asensio et al., 2013; Jiménez-Moreno et al., 2013). The development of zooxanthellate coral reefs in the nearby Sorbas Basin (W Mediterranean) during the late Messinian is consistent with this warming (Martín and Braga, 1994; Martín et al., 2010), but incompatible with the temperature range for the spawning of *M. modiolus* in the N Atlantic horse mussel reefs. Considering these notable ecological differences, aggregations of horse mussel can be ruled out as a recent analogue for the El Alcor mussel concentrations.

Massive accumulations of mollusks have also been described in the Mauritanian tropical shelf (NW Africa) under mesotrophic-eutrophic conditions linked to upwelling (Michel et al., 2011a, 2011b). These assemblages, overwhelmingly dominated by

ACCEPTED MANUSCRIPT

infaunal bivalves, are also highly diversified since nutrient-rich deep waters reaching the oceanic surface promote demographic blooms of primary producers that, in turn, support dense and diversified heterotrophic communities (Michel et al., 2011a, 2011b). The almost exclusive dominance of small mytilids in the El Alcor carbonates rules out their interpretation as shell concentrations in nutrient-rich areas, which are characterized by massive concentrations of diversified assemblages of infaunal bivalve, such as the ones on the Mauritanian shelf. Scarcity of infaunal benthic foraminifera typically related with upwelling areas, such as *Bolivina spathulata* (Mendes et al., 2004; Diz et al., 2006; Diz and Frances, 2008), disagrees with a nutrient-rich setting.

An alternative mechanism accounting for the origin of the El Alcor carbonates is cold-seep activity. Present-day cold-seep areas are colonized by chemosynthetic marine organisms and by microbial mats (Sibuet and Olu, 1998; Levin, 2005; Vanreusel et al., 2009). These chemosynthetic communities are characterized by low diversity (with only a few species dominating) but high-density populations (Rio et al., 1992; Sibuet and Olu, 1998; Levin, 2005; Hein et al., 2006; MacDonald et al., 2010). The El Alcor carbonates are densely packed and almost exclusively formed by small mytilids, in agreement with recent cold-seep communities.

Regarding benthic foraminiferal assemblages, recent cold-seep communities show no significant differences in diversity or density with respect to those of non-seep sites (e.g. Martin et al., 2010; Gieskes et al., 2011). Some recent cold-seep communities are dominated by a higher proportion of epifaunal as well as agglutinated species (Jones, 2006; Panieri and Sen Gupta, 2008; Martin et al., 2010; Panieri et al., 2014). Low diversity and high dominance is also observed in some fossil seep areas (Panieri, 2005; Martin et al., 2007; Panieri et al., 2009, 2012). Martin et al. (2007, 2010) and Panieri et al. (2014) also stressed that there are no endemic benthic foraminiferal

ACCEPTED MANUSCRIPT

communities linked to present-day cold-seep regions. In agreement with these findings, the benthic foraminiferal assemblages in the study area have characteristically low diversity and are dominated by *Biasterigerina planorbis* and *Cibicides refulgens*, two epifaunal species (Jorissen et al., 1995; Murray, 2006).

Present-day cold-seep assemblages form autochthonous-parautochthonous concentrations with highly fragmented but unabraded shells (Callender and Powell, 1992; Callender et al., 1992). In these particular settings, long-term exposure in the taphonomic active zone most likely accounts for the high fragmentation in low hydrodynamic settings. Particularly in most of the El Alcor upper subunit, small mytilid shells are fragmented but unabraded (Figs. 6A-6C). Therefore, most shells were accumulated in situ or nearby, with local reworking and transport, as indicated by the sedimentary structures.

The most destructive taphonomic process in cold-seep areas, as well as in hydrothermal vents, is dissolution (Paull and Neumann, 1987; Roux et al., 1989; Callender and Powell, 1992; Callender et al., 1992). However, chemosynthetic mussels have an outer calcitic layer (Génio et al., 2012) that increases shell-preservation potential. The small mytilids of the El Alcor carbonates preserve the calcitic layer while the aragonitic one (nacre layer) is dissolved (Figs. 7B-7C).

Both skeletal and authigenic non-skeletal carbonates in present-day as well as in fossil cold seeps can display a wide range of $\delta^{13}C$ values, from normal marine to very negative (Paull et al., 1985, 1989, 1992; Kulm et al., 1986; Río et al., 1986, 1992; Campbell, 1992; Gaillard et al., 1992; CoBabe, 1998; Hein et al., 2006; Campbell, 2006; Lietard and Pierre, 2009). We have analysed isotopes in bulk samples as well as carbonate shells of bivalves (small mytilids, *Neopycnodonte*, and pectinids), tubes of *Ditrupa* and benthic foraminiferal tests. The bulk samples collected at El Alcor

ACCEPTED MANUSCRIPT

carbonates reveal negative values for both carbon and oxygen isotopes (Table 2). The depletion in the isotope composition of these two elements, however, suggests a diagenetic imprint on the carbonates due to freshwater meteoric alteration (Hudson, 1977; Allen and Matthews, 1982; Lohmann, 1988; Nelson and Smith, 1996; Fisher et al., 2005).

Regarding the skeletal carbonates, the small mytilid shells register ^{13}C-depleted values as well as negative $\delta^{18}O$ values (Table 2, Fig. 8). Such values of carbon and oxygen isotopes point to diagenetic shell alteration. As commented above, the aragonitic (nacre) layer of the small mytilids was dissolved and blocky calcite was precipitated during diagenesis due to freshwater meteoric waters (Figs. 7B-7C). This alteration would account for the anomalous isotopic results. Nonetheless, there are two exceptions, i.e. samples CARANT-A and CARPARQ-2A, in which the isotopic signal seems to be unaltered (Table 2). Sample CARANT-A has $\delta^{13}C$ and $\delta^{18}O$ values of normal marine waters whereas sample CARPARQ-2A have carbon and oxygen values within the range of values reported by Paull et al. (1985, 1989, 1992) for cold-seep mussels from the Florida Escarpment (N Gulf of Mexico).

Oxygen isotopes in scallop shells reflect the $\delta^{18}O$ of marine waters since these organisms precipitate their shells in isotopic equilibrium (Roux et al., 1990). With respect to the carbon isotopes, however, ^{12}C enriches as the shell grows due to a vital effect (e.g. Lorrain et al., 2004). According to these authors, the $\delta^{13}C$ of juvenile shells of *Pecten maximus* ranges from -0.2 to +1.1‰, whereas adults show values ranging from ~ -1 to -0.1‰. Our results indicate that pectinid shells have anomalously negative $\delta^{13}C$ values (up to -5.4‰), far exceeding those due to the incorporation of light C during ontogeny (Table 2). ^{13}C-depleted waters released to the seafloor by cold seeps are dissolved into marine waters (Aharon et al., 1992; Valentine et al., 2001; Charlou et

ACCEPTED MANUSCRIPT

al., 2003; Lietard and Pierre, 2009). Organisms living in the proximity of seepages might precipitate their shells, incorporating light carbon isotopes in their carbonate skeletons directly from the seawater. Therefore, they have anomalously negative $\delta^{13}C$ values due to the influence of the oxidized methane fluids released into the water column (Beauchamp and Savard, 1992; Hein et al., 2006; Lietard and Pierre, 2009). Aharon et al. (1992) recorded values of up to -4.5‰ $\delta^{13}C$ of dissolved inorganic carbon in marine waters in the NW Gulf of Mexico. This value, together with the decrease in the $\delta^{13}C$ with scallop aging, agrees well with the values for the pectinids of El Alcor. Sample CARPARQ-1, however, shows very negative $\delta^{18}O$ level (Table 2), and therefore diagenesis due to meteoric water alteration cannot be completely ruled out.

Many authors have emphasized that the C isotopic composition of benthic foraminifera inhabiting cold seep is similar to that recorded in non-seep foraminifera (Sen Gupta and Aharon, 1994; Sen Gupta et al., 1997; Rathburn et al., 2000; Hill et al., 2003, 2004; Martin et al., 2004; Levin, 2005; Martin et al., 2007, 2010; Li et al., 2010; Gieskes et al., 2011; Panieri et al., 2014). However, dissolved inorganic carbon from pore waters at seep sites is highly enriched in ^{12}C. This means that benthic foraminifera inhabiting these settings precipitate their test in clear isotopic disequilibrium with the interstitial waters (e.g. Gieskes et al., 2011). Several interpretations have been proposed to account for the observed offset of C isotopic composition, but none satisfactorily explains the differences (Rathburn et al., 2000, 2003; Martin et al., 2004; Martin et al., 2007, 2010; Bernhard et al., 2010; Gieskes et al., 2011).

Despite the lack of a clear carbon-isotope signal, geochemical analyses have shown that carbon isotopes of benthic foraminifera in cold seeps display a wider range of variation than those living in normal marine settings (Sen Gupta et al., 1997; Rathburn et al., 2000, 2003; Hill et al., 2003, 2004; Martin et al., 2004; Martin et al.,

ACCEPTED MANUSCRIPT

2007, 2010; Bernhard et al., 2010; Gieskes et al., 2011; Panieri et al., 2014). In agreement with these observations, our results indicate a wide variation for $\delta^{13}C$ in the benthic foraminifera, from +0.32 to -3.5‰ (Table 2). The most negative values that we found fall within the same range of the most negative values found by Sen Gupta and Aharon (1994) and Sen Gupta et al. (1997) in recent cold-seep benthic foraminifers from the Gulf of Mexico, as well as by Li et al. (2010) from the Cascadian Margin, NE Pacific, and Panieri et al. (2014) in the Blake Ridge diapir, NE Atlantic Ocean.

In a methane seep at the Santa Barbara Channel (California), Hill et al. (2003) demonstrated that the $\delta^{13}C$ of benthic foraminifera varied from very negative to normal marine values just a few meters away from the main seepages. Additionally, Hill et al. (2004) studied the stable isotope composition of benthic foraminiferal shells associated with microbial mats and clam fields in the Hydrate Ridge, a cold-seep area off the Oregon coast (NE Pacific). They showed that the most $\delta^{13}C$-depleted values in benthic foraminifer tests correspond to those individuals inhabiting the microbial mats as a response to food source and/or the presence of microbial symbionts. Martin et al. (2004), however, found the most negative carbon isotopic values, up to -15.58‰, in benthic foraminifers inhabiting clam beds in the Clam Flat cold-seep chemosynthetic communities of Monterey Bay (California). Similarly, Panieri et al. (2014) revealed more negative values in benthic foraminifers associated with clam beds than in microbial mats of the Blake Ridge cold seep. The values of the benthic foraminifera inhabiting clam fields, both in Hydrate Ridge and Blake Ridge, were of the same magnitude and range as those found in the benthic foraminiferal assemblages associated with small mytilid-dominated carbonates of the El Alcor.

In the case of fossil cold seeps, early diagenetic processes might alter the original isotopic signal of benthic foraminiferal tests (Martin et al., 2004; Martin et al.,

ACCEPTED MANUSCRIPT

2007, 2010; Gieskes et al., 2011). In the study case, SEM analyses of benthic foraminifera show no secondary carbonate precipitation. However, cements can be overlooked (Martin et al., 2004; Martin et al., 2007, 2010) and, consequently, the isotopic signal can be slightly biased, accounting for the wide range of $\delta^{13}C$ variation. Nonetheless, it is well established that $\delta^{13}C$ is virtually unaffected during early diagenesis (Hudson, 1977; Dickson and Coleman, 1980; Jenkyns and Clayton, 1986; Madhavaraju et al., 2013).

The serpulid *Ditrupa* displays the most ^{13}C-depleted values (up to -16.1‰) but normal marine $\delta^{18}O$ values (Fig. 8, Table 2). Both carbon and oxygen isotopes of recent *D. arietina* tubes show normal marine values, from +1.48 to +1.8‰ and from +3.24 to +3.54‰, respectively (Table 2). Therefore, the highly depleted ^{13}C values in the El Alcor *Ditrupa* tubes are undoubtedly due to an extra supply of light carbon into the water column. This is the strongest geochemical evidence of cold-seep activity during the formation of the El Alcor carbonates. Considering a possible diagenetic bias, the studied *Ditrupa* tubes show no evident cements. Nonetheless, as mentioned above for benthic foraminifera, secondary carbonates could precipitate during diagenesis. In such a case, the diagenetic carbonate should be enriched primarily in ^{12}C, thus reinforcing the contention that the carbon source was most likely linked to seeps.

Recent cold seeps, as well as fossil counterparts, occur both in active and passive margins, associated with petroleum seeps, brine pools, mud volcanoes, and submarine fans (see summaries in Aharon 1994; Sibuet and Olu, 1998; Olu et al., 2004; Levin, 2005; Campbell, 2006; Olu et al., 2010). The El Alcor carbonates were deposited in the active margin of the Guadalquivir foreland basin (Fig. 1). As mentioned above, the marls at the base of the upper Miocene sediments rest on top of olistolithic deposits derived from the front nappes of the Betic Cordillera (Viguier, 1974; Perconig and

ACCEPTED MANUSCRIPT

Martínez-Díaz, 1977). Gas and oil exploration in the Carmona area has evidenced the presence of methane gas in the olistolithic deposits of the so-called Carmona nappe, as well as in the overlying Tortonian marls (Perconig and Martínez-Díaz, 1977; Álvarez, 1994; Martínez del Olmo and Mallo-García, 2002; Martínez del Olmo, 2004; Motis and Martínez del Olmo, 2013). Therefore, the seepage promoting the communities that produced the El Alcor carbonates could be related to methane emissions into the water column. Beds pervasively disrupted by fluid-escape structures in the Carmona Quarry section (Fig. 5) were probably the result of prolonged methane-rich fluids bubbling heterogeneously throughout the sediment into the water column. The size and shape of the studied carbonate body suggests the existence of a long front of a continuous, long-term seeping area in the outer platform at the southern basin margin, along the present-day El Alcor topographic high, which stimulated the profuse development of the small mytilid communities.

7.3. Comparison with other fossil cold-seep deposits

Major colonizers of present-day cold-seep areas include chemosynthetic marine bivalves (members of the families Mytilidae, Vesicomyidae, Lucinidae, Solemyidae, and Thyasiridae), followed by vestimentiferan worms, as well as microbial mats (Sibuet and Olu, 1998; Levin, 2005; Vanreusel et al., 2009). Together with the skeletal carbonate produced by mussels and associated chemosynthetic shelly organisms, authigenic carbonate production is mediated mostly by bacteria. All these carbonates have ^{13}C-depleted isotopic signal (see summaries in Sibuet and Olu, 1998; Schlager, 2003; Levin, 2005; Campbell, 2006; Taviani, 2010).

ACCEPTED MANUSCRIPT

Cold-seep metazoan assemblages in the fossil record since the Silurian (Barbieri et al., 2004) and possibly since the Cambrian (Campbell, 2006) have been recognized. The major components of these chemoautotrophous communities have changed over the Phanerozoic (Campbell and Bottjer, 1995; Van Dover et al., 2002; Little and Vrijenhoek, 2003; Peckmann and Goedert, 2005; Campbell, 2006; Taviani, 2010). Bivalves have been common cold-seep inhabitants since the Early Cretaceous onward, but they become particularly dominant during the Cenozoic (Campbell and Bottjer, 1995; Little and Vrijenhoek, 2003; Conti et al., 2010). Fossils in these communities usually cluster in the vicinity of fluid-seepage conduits although the lateral extension of fossil concentrations varies from tens to hundreds of meters.

In addition to the fossil assemblages, the main geochemical and sedimentary features of cold-seep areas have also remained constant through geological time (Campbell, 2006): 1) cold-seep deposits yield significant negative or widely variable $\delta^{13}C$ values; 2) typical deposits include microbial-mediated authigenic carbonate occurring as isolated patches or lenses in fine-grained siliciclastic sediment; 3) microbialites form thin crusts with a limited spatial distribution (about 1 m^2) close to the gas emissions; and 4) there are fluid-escape structures such as tubular concretions (e.g., Little and Vrijenhoek, 2003; Levin, 2005).

In our study case, variable to negative $\delta^{13}C$ shell values for different organisms and the presence of pervasive deformation structures due to fluid escape are consistent with typical cold-seep deposits. Nonetheless, the El Alcor carbonates differ in the rest of the features, making them an unusual sedimentary expression of cold seeps. They comprise a large-scale bioclastic body (dozens of kilometers) with neither authigenic micrite mud nor microbial crusts.

ACCEPTED MANUSCRIPT

Authigenic carbonate precipitation is mediated by methanotrophic and associated sulfate-reducing bacteria due to anaerobic oxidation of the methane (Ritger et al., 1987; Joye et al., 2010; Chevalier et al., 2011), even below the carbonate compensation depth (Greinert et al., 2002). This mechanism has been suggested for carbonate precipitation in fossil cold-seep-related deposits (e.g. Sibuet and Olu, 1998; Peckmann and Goedert, 2005). Major carbonate production in the El Alcor area, however, initially took place on a sandy, well-oxygenated bottom, as indicated by the dominance of epifaunal benthic foraminiferal species, and then continued on the gravelly sea floor provided by the accumulation of small mytilid shells. These conditions probably inhibited the anaerobic methanotrophic bacteria and might account for the absence of microbial carbonates.

Other unique features of the El Alcor carbonates include the geometry of fossil concentration and the most abundant components. Fossil cold-seep bivalve assemblages show low diversity and are characteristically dominated by large mytilids, lucinids, solemyids, vesicomyids, and thyasirids (e.g. Campbell, 2006; Taviani, 2010). They occur as fossil concentrations in isolated mound-like micritic floatstone intercalated within siliciclastic and referred to as chemoherms (Aharon, 1994; Roberts and Aharon, 1994; Majima et al., 2005). By contrast, the El Alcor carbonates form a continuous and homogeneous bioclastic body extending for dozens of square kilometers. Massive bubbling of methane throughout the entire El Alcor area might account for the extensive distribution of the small mussel-dominated carbonates. The pervasive presence of fluid-escape structures supports the idea of this widespread gas-release pattern.

In terms of taxonomic composition, chemosymbiont mytilid-dominated cold-seep communities are represented worldwide mostly by large *Bathymodiolus* (Distel et al., 2000; Campbell, 2006). The small representatives of ‘bathymodiolins’

ACCEPTED MANUSCRIPT

(*Benthomodiolus*, *Adipicola*, and *Idas*) are generally associated with sunken organic substrates, such as plant remains and vertebrate carcasses (Distel et al., 2000; Duperron et al., 2008; Lorion et al., 2010; Ritt et al., 2010, 2011, 2012). In the cases of *Idas* and *Adipicola*, the chemoautotrophic relationship with bacteria enables these mytilids to successfully thrive also in deep-sea cold seeps, such as in the Marmara Sea and the eastern Mediterranean, where they locally occur in dense populations around mud volcanoes and in the Nile deep-sea fan (Olu et al., 2004; Werne et al., 2004; Duperron et al., 2008; Brissac et al., 2011; Ritt et al., 2010, 2011, 2012). Therefore, the El Alcor carbonates might represent an exceptional example of massive colonization of a cold-seep setting by small mytilids, not yet either found in present-day cold seeps or reported from their fossil counterparts.

8. Conclusions

Upper Messinian bioclastic carbonates crop out in the El Alcor topographic high in the southern active margin of the Guadalquivir Basin (S Spain), the Betic foreland basin. The carbonates formed an isolated body up to 42 km long and up to 8 km across, surrounded by siliciclastic sediments. The carbonates can be divided into three subunits, corresponding from bottom to top to lowstand, transgressive, and highstand systems tract deposits, respectively, of a single depositional sequence. The limited distribution, the pervasive presence of trough cross-bedding and the mound-like geometry of the lower subunit suggest that it may represent a bar deposited in shallow waters. The intermediate subunit onlaps the previous deposits. Sediments are fine grained and exhibit parallel lamination, indicating that they were deposited in deeper water and under low-energy conditions. The upper subunit was deposited in a well-oxygenated

ACCEPTED MANUSCRIPT

outer platform setting, occasionally reached by storm waves, as evidenced by the presence of hummocky and swaley cross-stratification. Fluid-escape structures (pillars and dishes) are visible both in the upper subunit and in the lower one.

The carbonates are composed almost exclusively of small mytilids, resembling a group of chemosymbiont bivalves of the family Mytilidae. The dominance of these mytilids, together with variable to low $\delta^{13}C$ values (up to -16‰) of different skeletal carbonates (including benthic foraminifera, *Ditrupa* serpulids, small mytilids, *Neopycnodonte cochlear*, and pectinids), suggests that carbonate production most likely took place in a cold-seep area. The pervasive presence of fluid-escape structures points to gas release into the sea bottom from the underlying olistolithic deposits and marls. Carbonate components do not change along the outcrop, indicating continuous long-term gas bubbling along the outer platform, favoring profuse carbonate production due to massive development of the small mytilid communities in an otherwise terrigenous setting.

In contrast to other cold-seep deposits, the El Alcor carbonates comprise a large body homogeneously dominated by small mytilids deposited on well-oxygenated sediments, which inhibited authigenic carbonate precipitation. Therefore, the studied large bioclastic accumulation of the El Alcor topographic high seems to constitute an unusual sedimentary expression of cold-seep carbonates.

Acknowledgments

We acknowledge the review of two anonymous reviewers, which suggestions and comments have improved the quality of the manuscript. This paper has been supported by the research projects CGL2013-47236-P and Topo-Iberia Consolider

ACCEPTED MANUSCRIPT

Ingenio 2006 (CSD 2006-00041), both of the Ministerio de Ciencia e Innovación of Spain, and by Research Group RMN190 of the Junta de Andalucía. JNPA was funded by a research grant provided by the Ministerio de Educación of Spain (F.P.U. grant AP2007-00345). LG was supported by a postdoctoral fellowship from the Portuguese National Science Foundation (SFRH/BPD/96142/2013) founded by the Human Potential Operational Programme (POPH), inscribed in the National Strategic Reference Framework (QREN) and partially subsidized by the European Social Found. We specially acknowledge Drs Jordi Martinell and Rosa Domènech for the *Ditrupa* specimens from the Catalonian coast. We thank Christine Laurin and David Nesbit for the correction of the English text.

References

Aguirre, J., 1995. Implicaciones paleoambientales y paleogeográficas de dos discontinuidades estratigráficas en los depósitos pliocénicos de Cádiz (SW de España). Rev. Soc. Geol. España 8, 161-174.

Aguirre, J., 2000. Evolución paleoambiental y análisis secuencial de los depósitos plioceno de Almayate (Málaga, sur de España). Rev. Soc. Geol. España 13, 431-443.

Aguirre, J., Castillo, C., Férriz, F.J., Agustí, J., Oms, O., 1995. Marine continental magnetobiostratigraphic correlation of the *Dolomys* subzone (middle of Late Ruscinian): implications for the Late Ruscinian age. Palaeogeog., Palaeoclimatol., Palaeoecol. 117, 139-152.

Aharon, P., 1994. Geology and biology of modern and ancient submarine hydrocarbon seeps and vents: An introduction. Geo-Mar. Letters 14, 69-73.

ACCEPTED MANUSCRIPT

Aharon, P., Graber, E.R., Roberts, H.H., 1992. Dissolved carbon and $\delta^{13}C$ anomalies in the water column caused by hydrocarbon seeps on the northwestern Gulf of Mexico slope. Geo-Mar. Letters 12, 33-40.

Allen, J.R., Matthews, R.K., 1982. Isotope signatures associated with early meteoric diagenesis. Sedimentology 29, 797-817.

Álvarez, C., 1994. Hydrocarbons in Spain: exploration and production. First Break 12, 43-46.

Asmus, H., 1987. Secondary production of an intertidal mussel bed community related to its storage and turnover compartments. Mar. Ecol. Prog. Ser. 39, 251-266.

Baccelle, L., Bosellini, A., 1965. Diagrammi per la stima visiva della composizione percentuale nelle rocche sedimentary. Annali dell'Univ. Ferrara (Nuova Serie), Sez. 9, Sci. geol. paleontol. 1, 59-62.

Barbieri, R., Ori, G.G., Cavalazzi, B., 2004. A Silurian cold-seep ecosystem from the Middle Atlas, Morocco. Palaios 19, 527-542.

Beauchamp, B., Savard, M., 1992. Cretaceous chemosynthetic carbonate mounds in the Canadian Artic. Palaios 7, 434-450.

Berggren, W.A., Haq, B.U., 1976. The Andalusian stage (Late Miocene): Biostratigraphy, biochronology and paleoecology. Palaeogeog., Palaeoclimatol., Palaeoecol. 20, 67-129.

Bernhard, J.M., Martin, J.B., Rathburn, A.E., 2010. Combined carbonate carbón isotopic and cellular ultrastructural studies of individual benthic foraminifera: II. Towards an understanding of apparent disequilibrium in hydrocarbon seeps. Paleoceanography (PA4206). doi:10.1029/2010PA001930

Bertness, M.D., 1984. Ribbed mussels and *Spartina alterniflora* production in a New England salt marsh. Ecology 65,1794-1807.

ACCEPTED MANUSCRIPT

Bertness, M.D., Grosholz, E., 1985. Population dynamics of the ribbed mussel, *Geukensia demissa*: The cost and benefits of an aggregated distribution. Oecologia 67, 192-204.

Braga, J.C., Martín, J.M., Aguirre, J., 2002. Tertiary. Southern Spain, in: Gibbons, W., Moreno, T. (Eds.), The Geology of Spain. Geol. Soc., London, pp. 320-327.

Braga, J.C., Martín, J.M., Aguirre, J., Baird, C.D., Grunnaleite, I., Jensen, N.B., Puga-Bernabéu, A., Saelen, G., Talbot, M.R., 2010. Middle-Miocene (Serravallian) temperate carbonates in a seaway connecting the Atlantic Ocean and the Mediterranean Sea (North Betic Strait, S Spain). Sed. Geol. 225, 19-33.

Brissac, T., Rodrigues, C.F., Gros, O., Duperron, S., 2011. Characterization of bacterial symbioses in *Myrtea* sp. (Bivalvia: Lucinidae) and *Thyasira* sp. (Bivalvia: Thyasiridae) from a cold seep in the Eastern Mediterranean. Mar. Ecol. 32, 198-210.

Bromley, R.G., 1990. Trace fossils. Biology and taphonomy. Unwin Hyman, London.

Callender, W.R., Powell, E.N., 1992. Taphonomic signature of petroleum seep assemblages on the Louisiana upper continental slope: Recognition of autochthonous shell beds in the fossil record. Palaios 7, 388-408.

Callender, W.R., Powell, E.N., Staff, G.M., Davies, D.J., 1992. Distinguishing autochthony, parautochthony and allochthony using taphofacies analysis: Can cold seep assemblages be discriminated from assemblages of the nearshore and continental shelf? Palaios 7, 409-421.

Campbell, K.A., 1992. Recognition of a Mio-Pliocene cold seep setting from the northeast Pacific convergent margin, Washington, USA. Palaios 7, 422-433.

Campbell, K.A., 2006. Hydrocarbon seep and hydrothermal vent paleoenvironments and paleontology: Past developments and future research directions: paleoecology. Palaeogeog., Palaeoclimatol., Palaeoecol. 232, 362-407.

ACCEPTED MANUSCRIPT

Campbell, K.A., Bottjer, D.J., 1995. Brachiopods and chemosymbiotic bivalves in Phanerozoic hydrothermal vent and cold seep environments. Geology 23, 321-324.

Carter, J.G., 1990. Evolutionary significance of shell microstructure in the Palaeotaxodonta, Pteriomorphia and Isofilibranchia, in: Carter, J.G. (Ed.), Skeletal Biomineralization: Patterns, Process and Evolutionary Trends volume I. Van Nostrand Reinhold, New York, pp. 135-411.

Charlou, J.L., Donval, J.P., Zitter, P., Roy, N., Jean-Baptiste, P., Foucher, J.P., Woodside, J., 2003. Medinaut Scientific Party. Evidence of methane venting and geochemistry of brines on mud volcanoes of the eastern Mediterranean Sea. Deep-Sea Res., Part I 50, 941-958.

Chevalier, N., Bouloubassi, I., Birgel, D., Crémière, A., Taphanel, M.-H., Pierre, C., 2011. Authigenic carbonates at cold seeps in the Marmara Sea: (Turkey): A lipid biomarker and stable carbon and oxygen isotope investigation. Mar. Geol. 288, 112-121.

CoBabe, E.A., 1998. Chemosynthesis and chemosymbiosis in the fossil record: Detecting unusual communities using isotope geochemistry, in: Norris, R.D., Corfield, R.M. (Eds.), Isotope Paleobiology and Paleoecology. Paleontol. Soc. Papers 4, 255-285.

Commito, J.A., Dankers, N., 2001. Dynamics of spatial and temporal complexity in European and North American soft-bottom mussel beds, in: Reise, K. (Ed.), Ecological Comparisons of Sedimentary Shores. Springer-Verlag, Heidelberg, pp. 39–59.

Commito, J.A., Dow, W.E., Grupe, B.M., 2006. Hierarchical spatial structure in soft-bottom mussel beds. J. Exp. Mar. Biol. Ecol. 330, 27-37.

ACCEPTED MANUSCRIPT

Conti, S., Fontana, D., 2005. Anatomy of seep-carbonates: Ancient examples from the Miocene of the northern Apennines (Italy). Palaeogeog., Palaeoclimatol., Palaeoecol. 227, 156-175.

Conti, S., Fontana, D., Mecozzi, S., 2010. A contribution to the reconstruction of Miocene seepage from authigenic carbonates of the northern Apennines (Italy). Geo-Mar. Letters 30, 449-460.

Dam, G., 1990. Paleoenvironmental significance of trace fossils from the shallow marine lower Jurassic Neil Klinter Formation, East Greenland. Palaeogeog., Palaeoclimatol., Palaeoecol. 79, 221-248.

Dando, P.R., 2010. Biological communities at marine shallow-water vent and seep sites, in: Kiel, S. (Ed.), The Vent and Seep Biota. Aspects from Microbes to Ecosystems. Topics in Geobiology 33, Springer, pp. 333-378.

Dickson, J.A.D., Coleman, M.L., 1980. Changes in carbon and oxygen isotopic composition during limestone diagenesis. Sedimentology 27, 107-118.

Distel, D.L., Baco, A.R., Chuang, E., Morrill, W., Cavanaugh, C., Smith, C.R., 2000. Do mussels take wooden steps to deep-sea vents? Nature 403, 725-726.

Dittmann, S., 1990. Mussel beds – amensalism or amelioration for intertidal fauna? Helgoländer Meeresuntersuchungen 44, 335-352.

Diz, P., Francés, G., 2008. Distribution of live benthic foraminifera in the Ría de Vigo (NW Spain). Mar. Micropaleontol. 66, 165-191.

Diz, P., Francés, G., Rosón, G., 2006. Effects of contrasting upwelling–downwelling on benthic foraminiferal distribution in the Ría de Vigo (NW Spain). J. Mar. Systems 60, 1-18.

ACCEPTED MANUSCRIPT

Duperron, S., Halary, S., Lorion, J., Sibuet, M., Gaill, F., 2008. Unexpected co-occurrence of six bacterial symbionts in the gill of the cold seep mussel *Idas* sp. (Bivalvia: Mytilidae). Exp. Microbiol. 10, 433-446.

Elsäßer, B., Fariñas-Franco, J.M., Wilson, C.D., Kregting, L., Roberts, D., 2013. Identifying optimal sites for natural recovery and restoration of impacted biogenic habitats in a special area of conservation using hydrodynamic and habitats suitability modelling. J. Sea Res. 77, 11-21.

Fisher, J.K., Price, G.D., Hart, M.B., Leng, M.J., 2005. Stable isotope analysis of the Cenomanian-Turonian (Late Cretaceous) oceanic anoxic event in the Crimea. Cretac. Res. 26, 853-863.

Folmer , E.O., Drent, J., Troost, K., Büttger, H., Dankers, N., Jansen, J., van Stralen, M., Millat, G., Herlyn, M., Philippart, C.J.M., 2014. Large-scale spatial dynamics of intertidal mussel (*Mytilus edulis* L.) bed coverage in the German and Dutch Wadden Sea. Ecosystems 17, 550-566.

Franz, D.R., 1993. Allometry of shell and body weight in relation to shore level in the intertidal bivalve *Geukensia demissa* (Bivalvia: Mytilidae). J. Exp. Mar. Biol. Ecol. 174, 193-207.

Franz, D.R., 1996. Size and age at first reproduction of the ribbed mussel *Geukensia demissa* (Dillwyn) in relation to shore level in a New York salt marsh. J. Exp. Mar. Biol. Ecol. 205, 1-13.

Franz, D.R., 2001. Recruitment, survivorship, and age structure of a New York ribbed mussel population (*Geukensia demissa*) in relation to shore level—A nine year study. Estuaries 24, 319-327.

ACCEPTED MANUSCRIPT

Fürsich, F.T., Oschmann, W., Jaitly, A.K., Singh, I.B., 1991. Faunal response to transgressive-regressive cycles: examples from the Jurassic of western India. Palaeogeog., Palaeoclimatol., Palaeoecol. 85, 149-159.

Gaillard, C., Rio, M., Rolin, Y., Roux, M., 1992. Fossil chemosynthetic communities related to vents or seeps in sedimentary basins: The pseudobioherms of southeastern France compared to other world examples. Palaios 7, 451-465.

Génio, L., 2010. Systematics and evolutionary history of mytilids (Bivalvia) from chemosynthetic sites based on shell morphological characters. University of Leeds, Leeds, United Kingdom. 318 pp.

Génio, L., Kiel, S., Cunha, M.R., Grahame, J., Little, C.T.S., 2012. Shell microstructures of mussel (Bivalvia: Mytilidae: Bathymodiolinae) from deep-sea chemosynthetic sites: Do they have a phylogenetic significance? Deep-Sea Res., Part I 64, 86-103.

Gieskes, J., Rathburn, A.E., Martin, J.B., Elena Pérez, M., Mahn, C., Bernhard, J.M., Day, S., 2011. Cold seep in Monterey Bay, California: Geochemistry of pore waters and relationship to benthic foraminiferal calcite. App. Geochem. 26, 738-746.

González-Delgado, J.A., Civis, J., Dabrio, C.J., Goy, J.L., Ledesma, S., Pais, J., Sierro, F.J., Zazo, C., 2004. Cuenca del Guadalquivir, in: Vera, J.A. (Ed.), Geología de España, Soc. Geol. Esp. and IGME, Madrid, pp. 543-550.

Gormley, K.S.G., Porter, J.S., Bell, M.C., Hull, A.D., Sanderson, W.G., 2013. Predictive habitat modeling as a tool to assess the change in distribution and extent of an OSPAR priority habitat under and increased ocean temperature scenario: Consequences for marine protected area networks and management. PLoS ONE 8(7):e68263. doi:10.1371/journal.pone.0068263.

ACCEPTED MANUSCRIPT

Greinert, J., Bohrmann, G., Elvert, M., 2002. Stromatolitic fabric of authigenic carbonate crusts: results of anaerobic methane oxidation at cold seeps in 4,850 m water depth. Int. J. Earth Sc. 91, 671-698.

Gutiérrez, J.L., Jones, C.G., Strayer, D.L., Iribarne, O.O., 2003. Mollusks as ecosystem engineers: the role of shell production in aquatic habitats. Oikos 101, 79-90.

Hein, J.R., Normark, W.R., McIntyre, B.R., Lorenson, T.D., Powell, C.L., II., 2006. Methanogenic calcite, 13C-depleted bivalve shells, and gas hydrate from a mud volcano offshore southern California. Geology 34, 109-112.

Hill, T.M., Kennett, J.P., Spero, H.J., 2003. Foraminifera as indicators of methane-rich environments: A study of modern methane seeps in Santa Barbara Channel, California. Mar. Micropaleontol. 49, 123-138.

Hill, T.M., Kennett, J.P., Valentine, D.L., 2004. Isotopic evidence for the incorporation of methane-derived carbon into foraminifera from modern methane seeps, Hydrate Ridge, northeast Pacific. Geochim. Cosmochim. Acta 68, 4619-4627.

Hudson, J.D., 1977. Stable isotopes and limestone lithification. J. Geol. Soc. London 133, 637-660.

James, N.P., 1997. The cool-water carbonate depositional realm, in: James, N.P., Clarck, A.D. (Eds.), Cool-Water Carbonates. SEPM Spec. Publ., 56, 1-20.

Jenkyns, H.C., Clayton, C.J., 1986. Black shales and carbon isotopes in pelagic sediments from the Tethyan Lower Jurassic. Sedimentology 33, 87-106.

Jimenez-Moreno, G., Pérez-Asensio, J.N., Larrasoaña, J.C., Aguirre, J., Civis, J., Rivas-Carballo, M.R.R., Valle-Hernández, M.F., González-Delgado, J.A., 2013. Vegetation, sea-level, and climate changes during the Messinian salinity crisis. Geol. Soc. Am. Bull. 125, 432-444.

ACCEPTED MANUSCRIPT

Jones, R.W., 2006. Applied Micropalaeontology. Cambridge University Press, Cambridge, 434 pp.

Jorissen, F.J., de Stigter, H.C., Widmark, J.G.V., 1995. A conceptual model explaining benthic foraminiferal microhabitats. Mar. Micropaleontol. 26, 3-15.

Joye, S.B., Bowles, M.W., Samarkin, V.A., Hunter, K.S., Niemann, H., 2010. Biogeochemical signatures and microbial activity of different cold-seep habitats along the Gulf of Mexico deep slope. Deep-Sea Res. II 57, 1990-2001.

Kidwell, S.M., Holland, S.M., 1991. Field description of coarse bioclastic fabrics. Palaios 6, 426-434.

Kidwell, S.M., 1993. Taphonomic expressions of sedimentary hiatuses: Field observations on bioclastic concentrations and sequence anatomy in low, moderate and high subsidence settings. Geol. Rundschau 82, 189-202.

Kiel, S., Tyler, P.A., 2010. Chemosynthetical-driven ecosystems in the deep sea. In: Kiel, S. (Ed.), The Vent and Seep Biota. Aspects from Microbes to Ecosystems. Topics in Geobiology 33, Springer, pp. 1-14.

Kulm, L.D., Suess, E., Moore, J.C., Carson, B., Lewis, B.T., Ritger, S.D., Kadko, D.C. Thornberg, T.M., Embley, R.W., Rugh, W.D., Massoth, G.J., Langseth, M.R., Cochrane, G.R., Scamman, R., 1986. Oregon subduction zone: venting, fauna and carbonates. Science 231, 561-566.

Land, L.S., 1970. Phreatic versus meteoric diagenesis of limestones: evidence from a fossil water table. Sedimentology 14, 175-185.

Le Loc'h, F., Hily, C., Grall, J., 2008. Benthic community and food web structure on the continental shelf of the Bay of Biscay (North Eastern Atlantic) revealed by stable isotopes analysis. J. Mar. Systems 72, 17−34.

ACCEPTED MANUSCRIPT

Levin, L.A., 2005. Ecology of cold seep sediments: Interactions of fauna with flow, chemistry and microbes. Oceanog. Mar. Biol.: Annual Rev. 43, 1-46.

Lewis, D.W., Ekdale, A.A., 1992. Composite ichnofabric of a mid-Tertiary unconformity on a pelagic limestone. Palaios 7, 222-235.

Li, Q., Wang, J., Chen, J., Wei, Q., 2010. Stable carbon isotopes of benthic foraminifers from IODP expedition 311 as possible indicators of episodic methane seep events in a gas hydrate geosystem. Palaios 25, 671-681.

Lietard, C., Pierre, C., 2009. Isotopic signatures ($\delta^{18}O$ and $\delta^{13}C$) of bivalve shells from cold seeps and hydrothermal vents. Geobios 42, 209-219.

Lindenbaum, C., Bennell, J.D., Ress, E.I.S., McClean, D., Cook, W., Wheeler, E.J., Sanderson, W.G., 2008. Small-scale variation within *Modiolus modiolus* (Mollusca: Bivalvia) reef in the Irish Sea: I. Seabed mapping and reef morphology. J. Mar. Biol. Ass. UK. 88, 133-141.

Little, C.T.S., Vrijenhoek, R.C., 2003. Are hydrothermal vent animals living fossils? TRENDS Ecol. Evol. 18, 582-588.

Lohmann, K.C., 1988. Geochemical patterns of meteoric diagenetic systems and their application to paleokarst. In: Choquette, P.W., James, N.P. (Eds.), Paleokarst. Springer-Verlag, New York, pp. 58-80.

Loo, L.O., Rosenberg, R., 1983. *Mytilus edulis* culture: growth and production in western Sweden. Aquaculture 35, 137-150.

Lorion, J., Buge, B., Cruaud, C., Samadi, S., 2010. New insights into diversity and evolution of deep-sea Mytilidae (Mollusca: Bivalvia). Mol. Phylog. Evol. 57, 71-83.

Lorion, J., Kiel, S., Faure, B., Kawato, M., Ho, S.Y.W., Marshall, B., Tsuchida, S., Miyazaki, J.I., Fujiwara, Y., 2013. Adaptive radiation of chemosymbiotic deep-sea mussels. Proc. Royal Soc. B 280, 20131243. doi.org/10.1098/rspb.2013.1243.

ACCEPTED MANUSCRIPT

Lorrain, A., Paulet, Y.M., Chauvaud, L., Dunbar, R., Mucciarone, D., Fontugne, M., 2004. $\delta^{13}C$ variation in scallop shells: Increasing metabolic carbon contribution with body size? Geochim. Cosmochim. Acta 68, 3509-3519.

MacDonald, I.R., Smith, M., Huffer, F.W., 2010. Community structure comparisons of lower slope hydrocarbon seeps, northern Gulf of Mexico. Deep-Sea Res. II 57, 1904-1915.

Madhavaraju, J., Lee, Y.I., González-León, C.M., 2013. Diagenetic significance of carbon, oxygen and strontium isotopic compositions in the Aptian-Albian Mural Formation in Cerro Pimas area, northern Sonora, Mexico. J. Iberian Geol. 39, 73-88.

Magorrian, B.H., Service, M., 1998. Analysis of underwater visual data to identify the impact of physical disturbance on horse mussel (*Modiolus modiolus*) beds. Mar. Pollution Bull. 36, 354-359.

Majima, R., Nobuhara, T., Kitazaki, T., 2005. Review of fossil chemosynthetic assemblages in Japan. Palaeogeog., Palaeoclimatol., Palaeoecol. 227, 86-123.

Martin, J.B., Shelley, A.D., Rathburn, A.E., Elena Perez, M., Mahn, C., Gieskes, J., 2004. Relationships between the stable isotopic signatures of living and fossil foraminifera in Monterey Bay, California. Geochem., Geophys., Geosyst., 5, Q04004, doi:10.1029/2003GC000629.

Martín, J.M., Braga, J.C., 1994. Messinian events in the Sorbas Basin in southeastern Spain and their implications in the recent history of the Mediterranean. Sed. Geol. 90, 257-268.

Martín, J.M., Braga, J.C., Aguirre, J., Puga-Bernabéu, A., 2009. History and evolution of the North-Betic Strait (Prebetic Zone, Betic Cordillera): a narrow, early Tortonian, tidal-dominated, Atlantic–Mediterranean marine passage. Sed. Geol. 216, 80–90.

ACCEPTED MANUSCRIPT

Martín, J.M., Braga, J.C., Sánchez-Almazo, I.M., Aguirre, J., 2010. Temperate and tropical carbonate-sedimentation episodes in the Neogene Betic basins (southern Spain) linked to climatic oscillations and changes in Atlantic-Mediterranean connections: constraints from isotopic data. In: Mutti, M., Piller, W., Betzler, C. (Eds.). Carbonate Systems during the Oligocene-Miocene Climatic Transition. International Association of Sedimentologists Special Publication, Blackwell, Oxford, 42, 49-70.

Martin, R.A., Nesbitt, E.A., Campbell, K.A., 2007. Carbon stable isotopic composition of benthic foraminifera from Pliocene cold methane seeps, Cascadia accretionary margin. Palaeogeog., Palaeoclimatol., Palaeoecol. 246, 260–277.

Martin, R.A., Nesbitt, E.A., Campbell, K.A., 2010. The effects of anaerobic methane oxidation on benthic foraminiferal assemblages and stable isotopes on the Hikurangi Margin of Eastern New Zealand. Mar. Geol. 272, 270-284.

Martínez del Olmo, W., 2004. La exploración de hidrocarburos en el Terciario de España. Bol. Geol. Min. Esp. 115, 411-426.

Martínez del Olmo, W., Mallo-García, J.M., 2002. Non-renewable energy resources: oil and gas. In: Gibbons, W., Moreno, T. (Eds.), The Geology of Spain. Geological Society, London, pp. 494-499.

Mendes, I., Gonzalez, R., Dias, J.M.A., Lobo, F., Martins, V., 2004. Factors influencing recent benthic foraminifera distribution on the Guadiana shelf (Southwestern Iberia). Mar. Micropaleontol. 51, 171-192.

Michel, J., Vicens, G.M, Westphal, H., 2011a. Modern heterozoan carbonates from a eutrophic tropical shelf (Mauritania). J. Sed. Res. 81, 641-655.

ACCEPTED MANUSCRIPT

Michel, J., Westphal, H., van Cosel, R., 2011b. The mollusk fauna of soft sediments from the tropical, upwelling-influenced shelf of Mauritania (northwestern Africa). Palaios 26, 447-460.

Motis, K., Martínez del Olmo, W. 2013. Three different exploration plays in the marine Guadalquivir foreland basin in the context of the Late Miocene closure of the Thethys Ocean (south of Spain). AAPG European Regional Conference and Exhibition, Barcelona, Spain. Search and Discovery Article #10498 (2013).

Murray, J.W., 2006. Ecology and Applications of Benthic Foraminifera. Cambridge University Press, Cambridge.

Mutti, M., Hallock, P., 2003. Carbonate systems along nutrient and temperature gradients: smoe sedimentological and geochemical constraints. Int. J. Earth Sci. 92, 465-475.

Nelson, C.S., Smith, A.M., 1996. Stable oxygen and carbon isotope compositional fields for skeletal and diagenetic components in New Zealand Cenozoic nontropical carbonate sediments and limestones: a synthesis and review. New Zealand J. Geol. Geophys. 39, 93-107.

Olu, K., Cordes, E.E., Fisher, C.R., Brooks, J.M., Sibuet, M., Desbruyères, D., 2010. Biogeography and potential exchanges among the Atlantic equatorial belt cold-seep faunas. PLoS ONE 5, e11967, doi:10.1371/journal.pone.0011967.

Olu, K., Sibuet, M., Fiala-Médioni, A., Gofas, S., Salas, C., Mariotti, A., Foucher, J.P., Woodside, J., 2004. Cold seep communities in the deep eastern Mediterranean Sae: Composition, symbiosis and spatial distribution on mud volcanoes. Deep-Sea Res., Part I 51, 1915−1936.

Panieri, G., 2005. Benthic foraminifera associated with a hydrocarbon seep in the Rockall Trough (NE Atlantic). Geobios 38, 247–255.

ACCEPTED MANUSCRIPT

Panieri, G., Sen Gupta, B.K., 2008. Benthic foraminifera of the Blake Ridge hydrate mound, Western North Atlantic Ocean. Mar. Micropaleontol. 66, 91-102.

Panieri, G., Camerlenghi, A., Conti, S., Pini, G.A., Cacho, I., 2009. Methane seepages recorded in benthic foraminifera from Miocene seep carbonates, Northern Apennines (Italy). Palaeogeog., Palaeoclimatol., Palaeoecol. 284, 271–282.

Panieri, G., Camerlenghi, A., Cacho, I., Sanchez, Cervera C., Canals, M., Lafuerza, S., Herrera, G., 2012. Tracing seafloor methane emissions with benthic foraminifera: results from the Ana submarine landslide (Eivissa Channel, Western Mediterranean Sea). Mar. Geol. 291–294, 97–112.

Panieri, G., Aharon, P., Sen Gupta, B.K., Camerlenghi, A., Ferrer, F.P., Cacho, I., 2014. Late Holocene foraminifera of Blake Ridge diaper: Assemblage variation and stable-isotope record in gas-hydrate bearing sediments. Mar. Geol. 353, 99-107.

Paull, C.K., Neumann, A.C., 1987. Continental margin brine seeps: Their geological consequences. Geology 15, 545-548.

Paull, C.K., Jull, A.J.T., Toolin, L.J., Linick, T., 1985. Stable isotopic evidence for chemosynthesis in an abyssal seep community. Nature 315, 709-711.

Paull, C.K., Chanton, J.P., Neumann, A.C., Coston, J.A., Martens, C.S., 1992. Indicators of methane-derived carbonates and chemosynthetic organic carbon deposits: Examples from the Florida escarpment. Palaios 7, 361-375.

Paull, C.K., Martens, C.S., Chanton, J.P., Neumann, A.C., Coston, J., Jull, A.J.T., Toolin, L.T., 1989. Old carbon in living organisms and young $CaCO_3$ cements from abyssal brine seeps. Nature 342, 166-168.

Peckmann, J., Goedert, J.L., 2005. Geobiology of ancient and modern methane-seeps. Palaeogeog., Palaeoclimatol., Palaeoecol. 227, 1-5.

ACCEPTED MANUSCRIPT

Perconig, E., 1968. Biostratigrafia della sezione di Carmona (Andalusia, Spagna) in base ai foraminiferi planctonici. Giornale di Geol. 35, 191-218.

Perconig, E., Martínez-Díaz, C., 1977. Perspectivas petrolíferas de Andalucía occidental. Bol. Geol. Min. 88, 417-433.

Pérez-Asensio, J.N., Aguirre, J., Jiménez-Moreno, G., Schmiedl, G., Civis, J., 2013. Glacioeustatic control on the origin and cessation of the Messinian salinity crisis. Global Planet. Change 111, 1-8.

Pichler, T., Dix, G.R., 1996. Hydrothermal venting within a coral reef ecosystem, Ambitle Island, Papua New Guinea. Geology 24, 435-438.

Rathburn, A.E., Levin, L.A., Held, Z., Lohmann, K.C., 2000. Benthic foraminifera associated with cold seeps on the northern California margin: Ecology and stable isotopic composition. Mar. Micropaleontol. 38, 247-266.

Rathburn, A.E., Perez, M.E., Martin, J.B., Day, S.H., Mahn, C., Gieskes, J., Ziebis, W., Williams, D., Bahls, A., 2003. Relationships between the distribution and stable isotopic composition of benthic foraminifera and cold methane seep biogeochemistry in Monterey Bay, California. Geochem. Geophys. Geosyst. 4 1106. Doi: 10.1029/2003GC000595.

Ress, E.I.S., Sanderson, W.G., Mackie, A.S.Y., Holt, R.H.F., 2008. Small-scale variation within a *Modiolus modiolus* (Mollusca: Bivalvia) reef in the Irish Sea. III. Crevice, sediment infauna and epifauna from targeted cores. J. Mar. Biol. Ass. UK. 88, 151-156.

Rio, M., Roux, M., Renard, M., Herrera-Duvault, Y., Davanzo, F., Clauser, S., 1986. Fractionnement isotopique du carbone chez les bivalves dépendant d'une production primaire chimioautotrophe en milieu abyssal et littoral. Comp. R. l'Acad. Sci. Paris 303, 1553-1556.

ACCEPTED MANUSCRIPT

Rio, M., Roux, M., Renard, M., Schein, E., 1992. Chemical and isotopic features of present day bivalve shells from hydrothermal vents or cold seeps. Palaios 7, 351-361.

Ritger, S., Carson, B., Suess, E., 1987. Methane-derived authigenic carbonates formed by subduction-induced pore water expulsion along Oregon/Washington margin. Geol. Soc. Am. Bull. 98, 147-156.

Ritt, B., Serrazin, J., Caprais, J.-C., Noël, P., Gauthier, O., Pierre, C., Henry, P., Desbruyères, D., 2010. First insights into the structure and environmental setting of cold-seep communities in the Marmara Sea. Deep-Sea Res. I 157, 1120-1136.

Ritt, B., Pierre, C., Gauthier, O., Wenzhöfer, F., Boetius, A., Serrazin, J., 2011. Diversity and distribution of cold-seep fauna associated with different geological and environmental settings at mud volcanoes and pockmarks of the Nile deep-sea fan. Mar. Biol. 158, 1187-1210.

Ritt, B., Duperron, S., Lorion, J., Lazar, C.S., Serrazin, J., 2012. Integrative study of a new cold-seep mussel (Mollusca: Bivalvia) associated with chemosynthetic symbionts in the Marmara Sea. Deep-Sea Res. I 67, 121-132.

Roberts, H.H., Aharon, C.K., 1994. Hydrocarbon-derived carbonate build-ups of the northern gulf-of-mexico continental-slope. A review of submersible investigations. Geo-Mar. Letters 14, 135-148.

Roberts, H.H., Feng, D., Joye, S.B., 2010. Cold seep carbonates of the middle and lower continental slope, northern Gulf of Mexico. Deep-Sea Res. II 57, 2040-2054.

Roldán, F.J., 1995. Evolución neógena de la Cuenca del Guadalquivir. Ph.D. Thesis, University of Granada, Spain.

Roux, M., Rio, M., Schein, E., Lutz, R.A., Fritz, L.W. Ragone, L.M., 1989. Mesures in situ de la croissance des bivalves et des vestimentifères et de la corrosion des

ACCEPTED MANUSCRIPT

coquilles au site hydrothermal de 13ºN (dorsale du Pacifique oriental). Comp. R. l'Acad. Sci. Paris 308, 121-127.

Roux, M., Schein, E., Rio, M., Davanzo, F., Fily, A., 1990. Enregistrement des paramètres du milieu et des phases de croissance par les rapports 18O/16O et 13C/12C dans la coquille de Pecten maximus (Pectinidae, Bivalvia). Comp. R. l'Acad. Sci. Paris 304, 385-390.

Sanderson, W.G., Holt, R.H.F., Kay, L., Ramsay, K., Perrins, J., McMath, A.J., Rees, E.I.S., 2008. Small-scale variation within a *Modiolus modiolus* (Mollusca: Bivalvia) reef in the Irish Sea. II. Epifauna recorded by divers and cameras. J. Mar. Biol. Ass. UK. 88, 143-149.

Sanz de Galdeano, C., Vera, J.A., 1992. Stratigraphic record and paleogeographical contexto f the Neogene basins in the Betic Cordillera, Spain: Basin Rese. 4, 21−36.

Schlager, W., 2003. Benthic carbonate factories in the Phanerozoic. Inter. J. Earth Sci. 92, 445-464.

Sen Gupta, B.K., Aharon, P., 1994. Benthic foraminifera of bathyal hydrocarbon vents of the Gulf of Mexico: Initial report on communities and stable isotopes. Geo-Mar. Letters 14, 88−96.

Sen Gupta, B.K., Platon, E., Bernhard, J.M., Aharon, P., 1997. Foraminiferal colonization of hydrocarbon-seep bacterial mats and underlying sediment, Gulf of Mexico slope. J. Foram. Res. 27, 292-300.

Sibuet, M., Olu, K., 1998. Biogeography, biodiversity and fluid dependence of deep-sea cold-seep communities at active and passive margins. Deep-Sea Res., Part II 45, 517-567.

Sierro, F.J., González-Delgado, J.A., Dabrio, C.J., Flores, J.A., Civis, J., 1996. Late Neogene depositional sequences in the foreland basin of Guadalquivir (SW Spain),

ACCEPTED MANUSCRIPT

in: Friend, P., Dabrio, C.J. (Eds.), Tertiary Basins of Spain, Cambridge University Press, Cambridge, pp. 339–345.

Steuber, T., 2000. Skeletal growth rates of Upper Cretaceous rudist bivalves: implications for carbonate production and organism-environment feedbacks. Geol. Soc. London, Sp. Publ. 178, 21-32.

Taviani, M., 2010. The deep-sea chemoautotroph microbial world as experienced by the Mediterranean metazoans through time, in: Reitner et al. (Eds.), Advances in Stromatolite Geobiology, Springer-Verlag, Berlin. Lecture Notes in Earth Sciences 131, 277-295.

Taylor, J.D., Kennedy, W.J., Hall, A., 1969. The shell structure and mineralogy of the Bivalvia. Introduction, Nuculacea-Trigonacea. Bull. Br. Mus. Nat. Hist. (Zool.) Suppl. 3, 1-125.

Thubaut, J., Puillandre, N., Faure, B., Cruaud, C., Samadi, S., 2013. The contrasted evolutionary fates of deep-sea chemosynthetic mussels (Bivalvia, Bathymodiolinae). Ecol. Evol. 1-19. doi: 10.1002/ece3.749.

Valentine, D.L., Blanton, D.C., Reburgh, W.S., Kastner, M., 2001. Water column methane oxidation adjacent to an area of active hydrate dissociation, Eel River Basin. Geochim. Cosmochim. Acta 65, 2633-2640.

Van Dover, C.L., German, C.R., Speer, K.G., Parson, L.M., Vrijenhoek, R.C., 2002. Evolution and biogeography of deep-sea vent and seep invertebrates. Science 295, 1253-1257.

Vanreusel, A., Andersen, A.C., Boetius, A., Connelly, D., Cunha, M.R., Decker, C., Hilario, A., Kormas, K.A., Maignien, L., Olu, K., Pachiadaki, M., Ritt, B., Rodrigues, C., Sarrazin, J., Tyler, P., van Gaever, S., Vanneste, H., 2009.

ACCEPTED MANUSCRIPT

Biodiversity of cold seep ecosystems along the European margins. Oceanography 22, 110-127.

Viguier, C., 1974. Le Néogène de l'Andalousie nord-occidentale (Espagne). Histoire géologique du «Bassin du Bas Guadalquivir». Ph.D. Thesis, University of Bordeaux, France.

Werne, J.P., Haese, R.R., Zitter, T., Aloisi, G., Bouloubassi, I., Fiala-Médiconi, A., Pancost, R.D., Sinninghe Damsté, J.S., de Lange, G., Forney, L.J., Gottschal, J.C., Foucher, J.P., Mascle, J., Woodside, J., 2004. Life at cold seeps: a synthesis of biogeochemical and ecological data from Kazan mud volcano, eastern Mediterranean Sea. Chem. Geol. 205, 367-390.

Wildish, D.J., Fader, G.B.J., 1998. Pelagic-benthic coupling in the Bay of Fundy. Hydrobiologia 375/376, 369-380.

Wildish, D.J., Fader, G.B.J., Parrot, D.R., 2009. A model of horse mussel reef formation in the Bay of Fundy based on population growth and geological processes. Atl. Geol. 45, 157-170.

Wildish, D.J., Fader, G.B.J., Lawton, P., MacDonald, A.J., 1998. The acoustic detection and characteristics of sublittoral bivalve reefs in the Bay of Fundy. Cont. Shelf Res. 18, 105-113.

Wilson, B., 1998. Order Mytiloida. in: Beesley, P.L., Ross, G.J.B., Wells, A. (Eds.), Mollusca: The Southern Synthesis. Fauna of Australia. Vol. 5, CSIRO Publishing, Melbourne, Part A. 250-253.

Wissak, M., López Correa, M., Gofas, S., Salas, C., Taviani, M., Jakobsen, J., Freiwald, A., 2009. Shell architecture, element composition, and stable isotope signature of the giant deep-sea oyster *Neopycnodonte zibrowii* sp. nov. from the NE Atlantic. Deep-Sea Res. I 56, 374-407.

ACCEPTED MANUSCRIPT

Figure captions

Figure 1. Simplified geological sketch of the Betic Cordillera and geological map of the study area. Numbers indicate the location of the four studied stratigraphic sections: 1- Carmona Quarry, 2- Carmona Antena, 3- Carmona Fútbol, 4- Alcalá de Guadaira.

Figure 2. Stratigraphic logs with indication of the position of the samples used for isotope analyses and benthic foraminiferal assemblage determinations. Samples labeled CARPARQ in the Carmona Antena section were collected in a parallel section, located 500 m to the SW of Carmona Antena section, which exhibits the same stratigraphic and sedimentologic features. L.S. = Lower subunit; I.S. = Intermediate subunit; U.S. Upper subunit.

Figure 3. **A**) North-South and **B**) West-East panoramic views of the three subunits of the studied carbonates in the Carmona Quarry section.

Figure 4. Some significant sedimentary features in the studied deposits. **A**) Trough cross-bedding (lower subunit, Carmona Quarry section). **B**) Slump (lower subunit, Carmona Quarry section). **C**) Intensely bioturbated silty/sandy packstones at the uppermost part of the intermediate subunit in the Carmona Antena section. **D**) Field view of the intermediate subunit in the Carmona Fútbol section. Person sitting in one of the fine-grained sandy packstone intercalations. **E**) Hummocky and swaley cross-stratification (upper subunit, Carmona Fútbol section).

ACCEPTED MANUSCRIPT

Figure 5. Fluid-scape structures in the upper subunit (Carmona Quarry section). **A**) Field-view of highly deformed strata. The white arrow points to a fluid-escape shaft seen in cross-section. Man for scale is 1.75 m tall. **B**) Detailed view of the inset in previous picture. Arrows point to fluid-escape channels. **C**) Pervasively deformed strata. Deformation is probably the result of methane bubbling throughout the carbonates. **D**) Sediment deformation around a fluid-escape conduit (arrow).

Figure 6. Major components of the El Alcor carbonates. **A**) Close-up field view of the carbonates. Small mytilid fragments predominate, the vast majority of them having sharp edges, indicating the absence of abrasion. **B**-**C**) Nearly complete shells of small mytilids. Note that commarginal growth lines are clearly visible. **D**-**E**) Casts of two complete individuals of small mytilids. Growth lines are visible.

Figure 7. Microphotographs of small mytilids. **A**) SEM photograph showing the characteristic edentulous hinge. **B**) Microphotograph of the El Alcor carbonates showing non-abraded small mytilid fragments. Note that the calcite fibrous prismatic outer layer of the shells is well preserved, whereas the inner layer has been dissolved and the subsequent void filled up by sparry, blocky calcite. **C**) SEM photograph showing the ultrastructure of small mytilid shells. **D**-**E**) Detailed views of the fibrous prismatic outer layer of the specimen in Fig. 7C.

Figure 8. Carbon and oxygen isotope data of the analyzed samples (isotope raw data in Table 2). *Ditrupa* worm tubes show the most negative $\delta^{13}C$ values.

ACCEPTED MANUSCRIPT

Figure 9. Sketch showing the sequence stratigraphic framework of the three subunits and the relative position of the studied sections.

ACCEPTED MANUSCRIPT

ACCEPTED MANUSCRIPT

Table captions

Table 1. Raw data (number of specimens of the different species) for the benthic foraminiferal assemblages. Most abundant species (>3% of the total assemblages) are indicated in bold.

Table 2. Carbon and oxygen stable isotope raw data. Sample labels as in Fig. 2, except those indicated with the asterisks, which refer to the present-day *Ditrupa arietina* from the Cabo de Gata (LP) and Sant Feliu de Gruixols (SFG). Samples labeled as Neo1 to Neo4 correspond to *Neopycnodonte* shells collected from the sample CARPARQ-2. Samples labeled as Chim1 to Chim5 correspond to bulk samples collected from fluid-scape conduits in the middle part of the upper subunit of Carmona Quarry section.

ACCEPTED MANUSCRIPT

ACCEPTED MANUSCRIPT

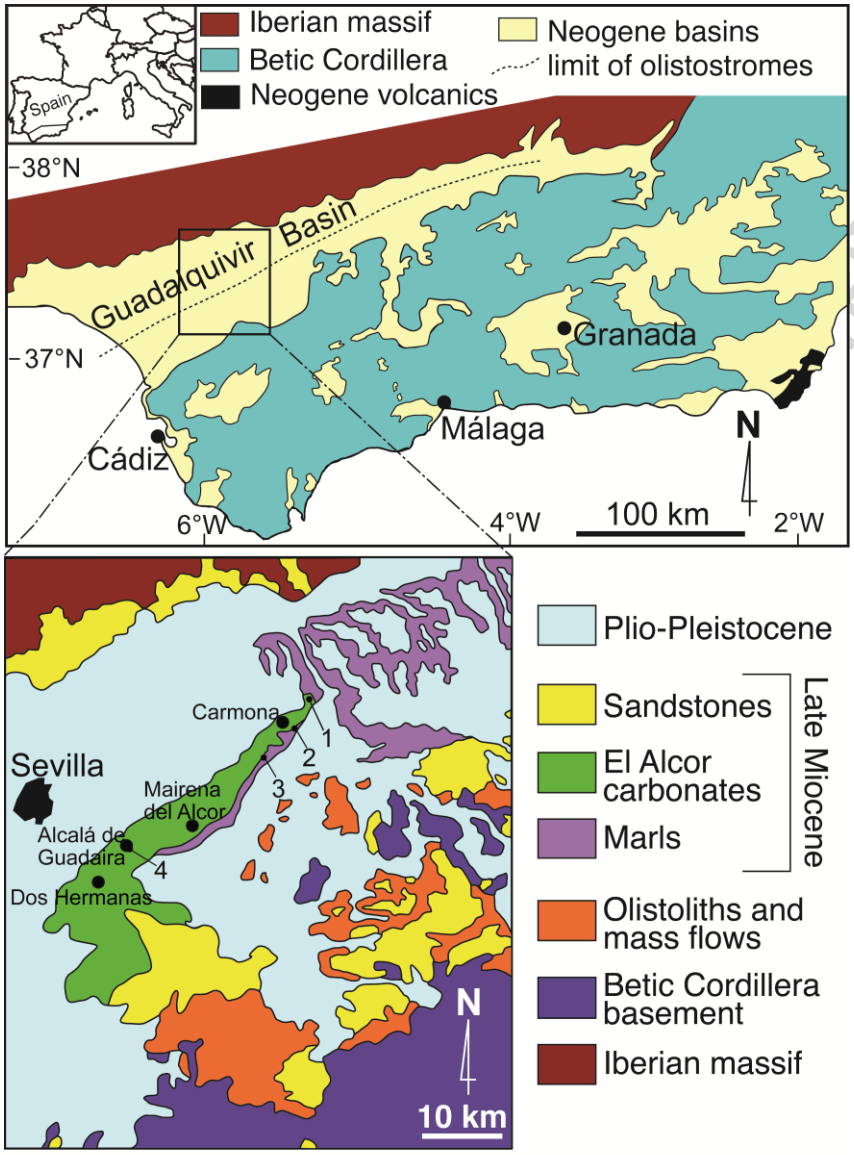

Fig. 1

ACCEPTED MANUSCRIPT

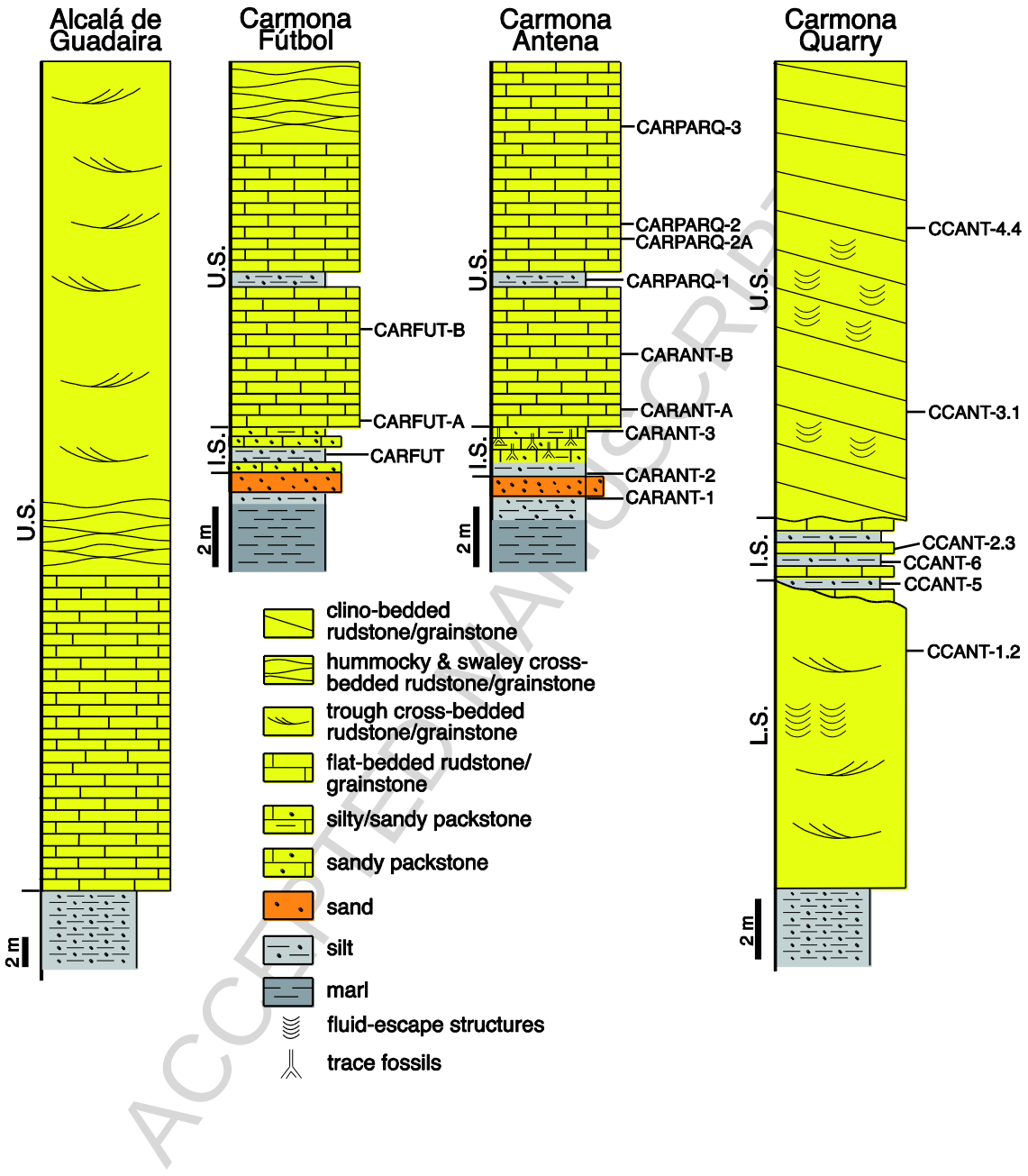

Fig. 2

ACCEPTED MANUSCRIPT

Figure 3

ACCEPTED MANUSCRIPT

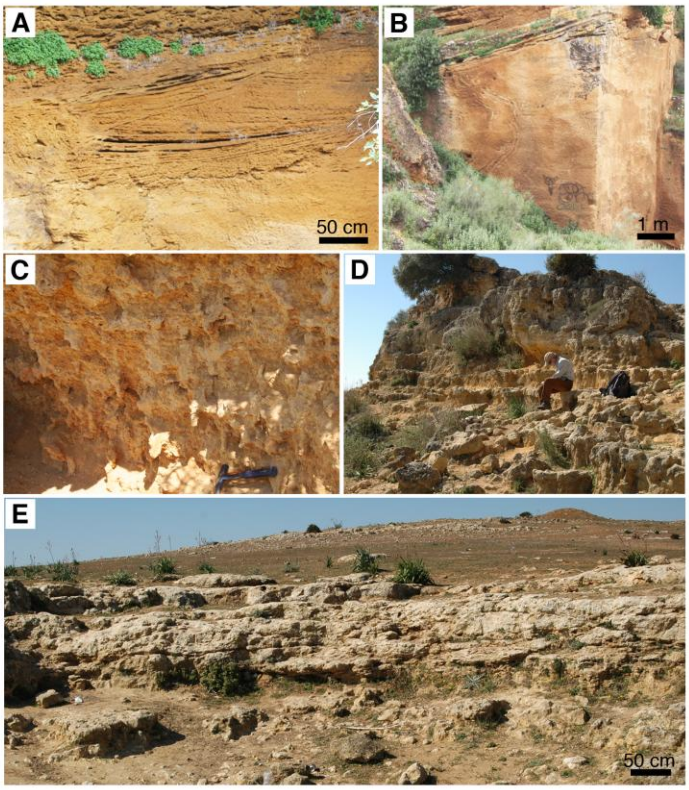

Figure 4

ACCEPTED MANUSCRIPT

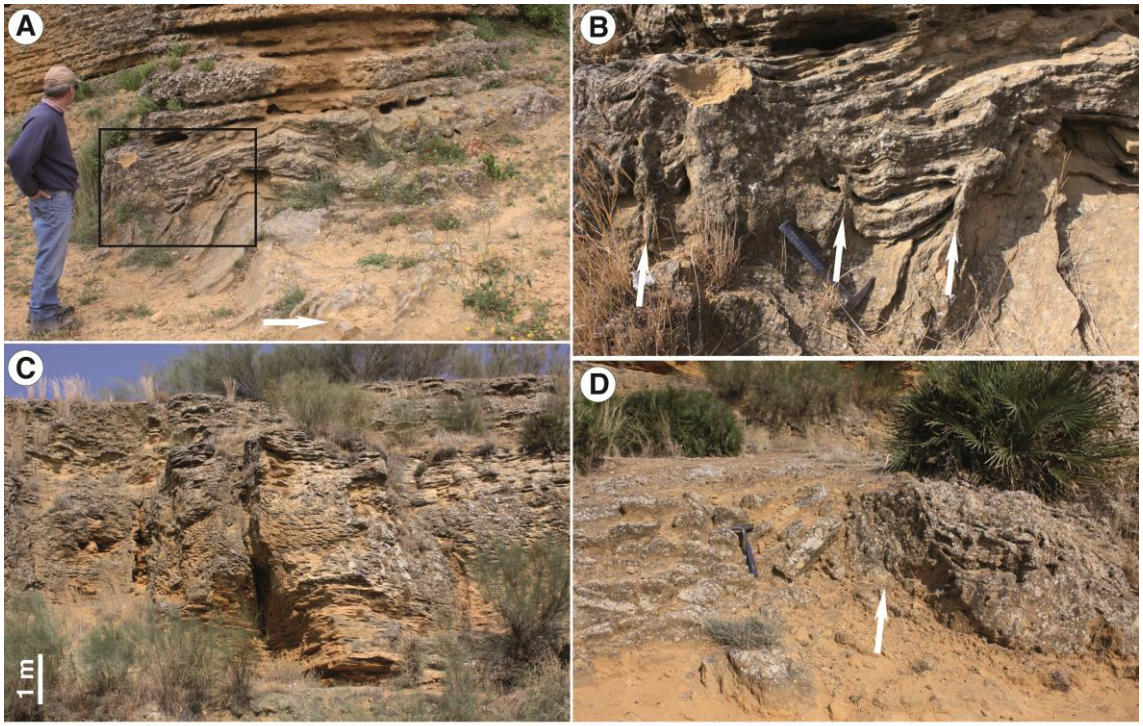

Fig. 5

ACCEPTED MANUSCRIPT

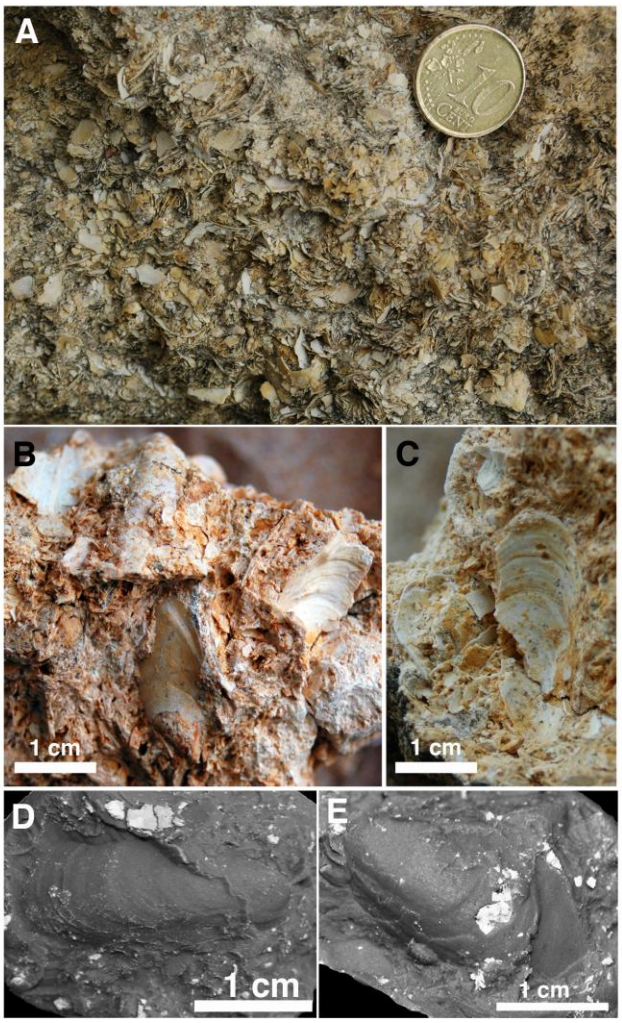

Fig. 6

ACCEPTED MANUSCRIPT

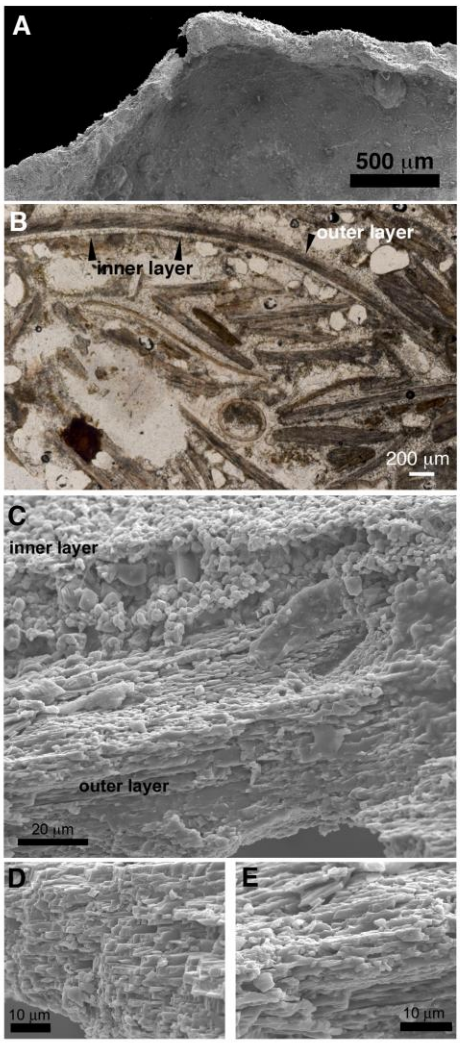

Fig. 7

ACCEPTED MANUSCRIPT

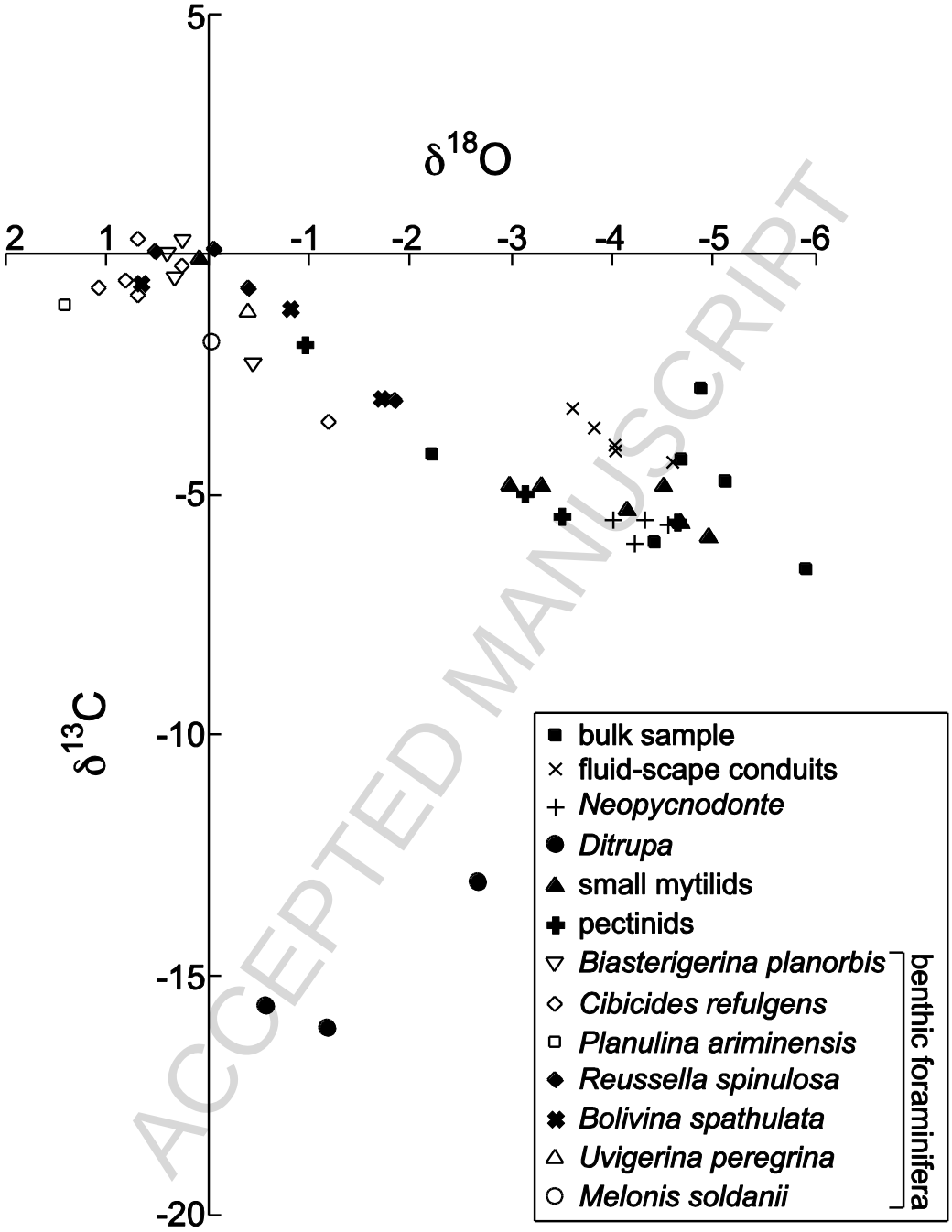

Figure 8

ACCEPTED MANUSCRIPT

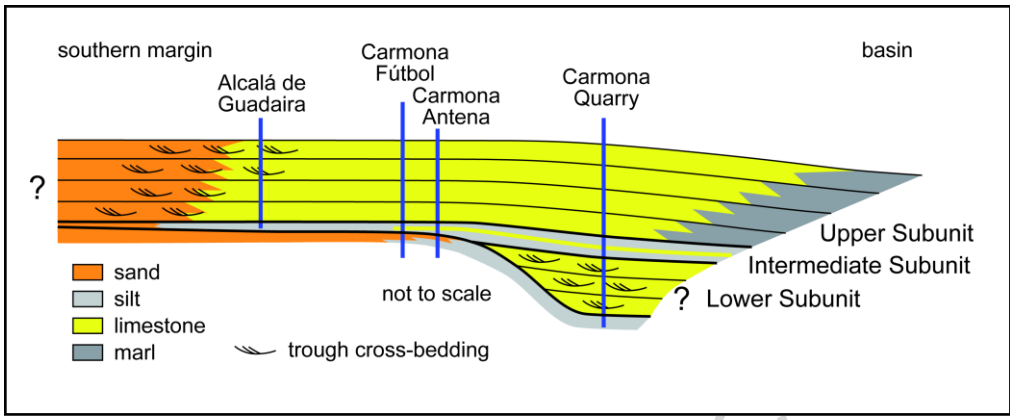

Fig. 9

ACCEPTED MANUSCRIPT

ACCEPTED MANUSCRIPT

Table 1

	CARANT-1	CARANT-2	CARANT-3	CARPARQ-1	CARFUT	CCANT-5	CCANT-6
Ammonia beccarii	1	2	5	1	12		10
Ammonia inflata		1					28
Ammonia sp.	3	3	3	6	5	1	3
Amphicoryna scalaris		3		1			1
Anomalina flinti							
Biasterigerina planorbis	75	84	52	66	57	63	5
Asterigerinata sp.	5						
Bolivina earlandi		1	1				
Bolivina reticulata	1						
Bolivina dilatata		1	2		1	5	
Bolivina spathulata	15	3	16	4	11	24	
Bolivina sp.	1		1	1			3
Bulimina aculeata	1		1	1	2	1	11
Bulimina elongata			2	1	3	2	1
Bulimina striata	1	1		1	1	3	3
Bulimina sp.							7
Cancris auriculus				3			
Cancris sp.	2				1	2	
Cassidulina sp.		1					
Evolvocassidulina bradyi		1			2		
Lobatula lobatula	22	18	11	7	7	1	
Cibicides refulgens	50	54	51	76	54	55	1
***Cibicides* sp. 1**	11	5	11	5	8		
***Cibicides* sp. 2**	15	10	16	18	14	15	3
Cibicides dutemplei	2	10	6	5	5	4	23
Cibicides pachyderma	4	8	4	1	9	17	39
Cibicides ungerianus		2	3		1		1
***Cibicides* sp.**	11	8	6	13	14	14	14
Dentalina sp.			1				
Bannerella gibbosa				1	1		
Elphidium advenum	1	2	5		4	4	
Elphidium complanatum	8	14	5	7		2	
Elphidium crispum	3	1	4	7	2		
Elphidium granosum			1				
Elphidium macellum	10	2		2	1		
Elphidium translucens				1			
Elphidium sp.						4	
Epistominella sp.					1		
Globobulimina sp.		1					
Globocassidulina subglobosa			2			4	
Globulina sp.			1	1			
Gyroidina umbonatus	1	1	1		1		

ACCEPTED MANUSCRIPT

Gyroidina sp.			1	1		2	
Hanzawaia boueana	16	15	26	16	21	20	2
Haynesina depressula	1						
Haynesina sp.			1				
Hoeglundina elegans					1		
Lagena sp.			2		1		
Lenticulina sp.	1	1	2	2	2	3	1
Marginulinopsis costata		1		1			
Marginulina sp.						1	
Martinottiella communis		1					9
Melonis barleeanum							2
Melonis pompilioides	1					1	19
Melonis sp.						4	8
Neoconorbina terquemi	1						
Neoeponides schreibersii					1		21
Neoeponides sp.	1		1				
Nodosaria sp.	4	6	4	5	5	2	2
Elphidium fabum	5		8	5	9	5	3
Nonion sp.		1	3		5	6	
Nonionella sp.					1		
Oridorsalis umbonatus	1		1		4		
Planulina ariminensis	1	7	1	4	2	1	52
Planulina sp.	1				3		
Poroeponides sp.	1						
Pullenia bulloides		1	2	1	3	3	9
Pullenia quinqueloba							2
Uvigerina bononiensis					1	1	
Reussella spinulosa	13	19	24	22	16	11	
Rosalina sp.			1		2	2	
Sphaeroidina bulloides		2	2	1		2	
Spiroplectinella wrightii	5	8	6	7	2		6
Siphonodosaria lepidula							1
Sahulia conica	3	1	1	4	1	1	
Textularia sp.			1			2	1
Trifarina angulosa	1		2		2	9	
Trifarina bradyi	1				1		
Uvigerina peregrina				2		3	3
Uvigerina sp.							6
Total	300	300	300	300	300	300	300

ACCEPTED MANUSCRIPT

Table 2

Sample	$\delta^{13}C$	$\delta^{18}O$	Carbonate source
CARANT-2	-13.028	-2.672	*Ditrupa*
CARANT-2	-16.1	-1.17	*Ditrupa*
CARANT-2	-15.654	-0.558	*Ditrupa*
CARPARQ-2A	-4.809	-2.983	Small mytilid
CARANT-B	-5.549	-4.685	Small mytilid
CARPARQ-3	-5.86	-4.95	Small mytilid
CARPARQ-2	-4.79	-4.52	Small mytilid
CARPARQ-1	-5.33	-4.14	Small mytilid
CARANT-A	-0.10	0.08	Small mytilid
CARFUT-B	-4.82	-3.30	Small mytilid
CARPARQ-1	-4.973	-3.131	Pectinid
CARPARQ-1	-5.428	-3.504	Pectinid
CARPARQ-1	-5.57	-4.65	Pectinid
CARANT-A	-1.84	-0.95	Pectinid
Neo1	-5,46	-4,39	*Neopycnodonte*
Neo2	-5,45	-4,01	*Neopycnodonte*
Neo3	-6,03	-4,27	*Neopycnodonte*
Neo4	-5,58	-4,42	*Neopycnodonte*
CCANT-3.1	-2.76	-4.86	Bulk sample
CARPARQ-2	-6.55	-5.92	Bulk sample
CARFUT-A	-4.16	-2.22	Bulk sample
CCANT-1.2	-4.71	-5.11	Bulk sample
CCANT-2.3	-4.26	-4.67	Bulk sample
CCANT-4.4	-5.97	-4.42	Bulk sample
Chim1	-4,541	-4,638	Fluid-scape conduit
Chim2	-3,548	-3,636	Fluid-scape conduit
Chim3	-3,89	-3,969	Fluid-scape conduit
Chim4	-4,032	-4,102	Fluid-scape conduit
Chim5	-3,726	-3,787	Fluid-scape conduit
CARANT-1	0.32	0.26	*Biasterigerina planorbis*
CARANT-1	0.06	0.52	*Reussella spinulosa*
CARANT-1	0.31	0.69	*Cibicides refulgens*
CARANT-1	-0.59	0.66	*Bolivina spathulata*
CARANT-2	-0.41	-1.35	*Biasterigerina planorbis*
CARANT-2	-0.55	0.82	*Cibicides refulgens*
CARANT-2	0.1	-0.05	*Reussella spinulosa*
CARANT-2	-1.1	-0.8	*Bolivina spathulata*
CARANT-3	0.01	0.404	*Biasterigerina planorbis*
CARANT-3	-0.24	0.25	*Cibicides refulgens*
CARPARQ-1	-2.27	-0.45	*Biasterigerina planorbis*
CARPARQ-1	-3.5	-1.2	*Cibicides refulgens*
CARPARQ-1	-3.04	-1.85	*Reussella spinulosa*

ACCEPTED MANUSCRIPT

CARPARQ-1	-2.96	-1.71	*Bolivina spathulata*
CARFUT	-0.47	0.33	*Biasterigerina planorbis*
CARFUT	-0.85	0.7	*Cibicides refulgens*
CARFUT	-0.67	-0.4	*Reussella spinulosa*
CCANT-6	-0.67	1.07	*Cibicides dutemplei*
CCANT-6	-1.03	1.43	*Planulina ariminensis*
CCANT-6	-1.83	-0.04	*Melonis pompilioides*
CCANT-6	-1.18	-0.39	*Uvigerina peregrina*
LP2-60*	1.48	3.29	*Ditrupa arietina*
LP4-60*	1.63	3.4	*Ditrupa arietina*
LP2-50*	1.80	3.24	*Ditrupa arietina*
SFG-1*	1.74	3.54	*Ditrupa arietina*

ACCEPTED MANUSCRIPT

ACCEPTED MANUSCRIPT

An enigmatic kilometre-scale concentration of small mytilids (Late Miocene, Guadalquivir Basin, S Spain)

Julio Aguirre, Juan C. Braga, José M. Martín, Ángel Puga-Bernabéu, José N. Pérez-Asensio, Isabel M. Sánchez-Almazo and Luciana Génio

Highlights

- Heterozoan carbonates crop out in the S margin of the Guadalquivir Basin (S Spain)
- They form a narrow belt surrounded by terrigenous in the El Alcor topographic high
- 95% of the skeletal components are small mytilids
- Negative C isotopes of *Ditrupa* shells and fluid-scape structures are pervasive
- The carbonate body of El Alcor is interpreted as an unusual cold-seep deposit

ACCEPTED MANUSCRIPT